

Green Chemistry

Accepted Manuscript



This is an *Accepted Manuscript*, which has been through the Royal Society of Chemistry peer review process and has been accepted for publication.

Accepted Manuscripts are published online shortly after acceptance, before technical editing, formatting and proof reading. Using this free service, authors can make their results available to the community, in citable form, before we publish the edited article. We will replace this *Accepted Manuscript* with the edited and formatted *Advance Article* as soon as it is available.

You can find more information about *Accepted Manuscripts* in the [Information for Authors](#).

Please note that technical editing may introduce minor changes to the text and/or graphics, which may alter content. The journal's standard [Terms & Conditions](#) and the [Ethical guidelines](#) still apply. In no event shall the Royal Society of Chemistry be held responsible for any errors or omissions in this *Accepted Manuscript* or any consequences arising from the use of any information it contains.

Hydroxyl ammonium ionic liquids as media for biocatalytic oxidations

Athena A. Papadopoulou,^a Andromachi Tzani,^b Dimitrios Alivertis,^a Maria H. Katsoura,^a Angeliki C. Polydera,^a Anastasia Detsi,^b and Haralambos Stamatis^{a*}

Cite this: DOI: 10.1039/x0xx00000x

Received 00th January 2012,
Accepted 00th January 2012

DOI: 10.1039/x0xx00000x

www.rsc.org/

In this work, neoteric and biodegradable ionic liquids (ILs) based on various hydroxyl ammonium cations and formic acid anion have been used as media for biocatalytic oxidoreductions catalyzed by different metalloproteins. The effect of these ILs on the biocatalytic behavior and structure of solubilized enzymes was investigated using cytochrome c (cyt c) as a model protein. The use of ILs-based media enhances the tolerance of cyt c against the denaturing effect of H₂O₂ and increases (up to 20 fold) its catalytic efficiency compared to that observed in buffer. This beneficial effect strongly correlates with the concentration of ILs used, as well as the chaotropicity of their cations. UV-vis, circular dichroism and Fourier transform infrared (FT-IR) spectroscopic studies indicated that, the effect of ILs on the catalytic behavior of cyt c could be correlated with slight structural changes on the protein molecule and/or perturbations of the heme microenvironment. The use of hydroxyl ammonium-based ILs as reaction media increased (up to 4-fold) the decolorization activity of cyt c. All ILs used were recycled and successfully reused three times indicating the potential application of these novel ILs as environmentally friendly media for biocatalytic processes of industrial interest.

1 Introduction

2 Ionic liquids (ILs), also called molten salts, are
3 mixtures of cations and anions that melt below 100 °C and
4 have received considerable attention over the last decade as an
5 environmentally friendly alternative to organic solvents. Due to
6 their interesting physical and chemical properties, such as
7 negligible vapour pressure, ability to dissolve various
8 hydrophobic/hydrophilic compounds and excellent chemical
9 and thermal stability, they have been widely used as “green”
10 media for biocatalytic processes.¹⁻³ The first studies of enzyme-
11 catalyzed reactions in ILs were reported in so called second
12 generation ILs, which are mainly based on cations of
13 heterogeneous cyclic amines, such as substituted imidazoliums
14 and alkyl pyridiniums, as well as poor nucleophilic anions,
15 such as (BF₄)⁻, (PF₆)⁻, (CF₃CO₂)⁻, (CF₃SO₃)⁻.⁴⁻⁶

16 In the last years, numerous studies of second
17 generation ILs, in the context of biocatalysis, revealed that
18 many enzymes exhibit excellent selectivity and activity and
19 maintain very high thermal and operational stability in these
20 solvents.⁶⁻¹² However, their use in large scale applications is
21 limited due to their difficult preparation and high cost.¹
22 Moreover, concerns have arisen regarding the environmental

23 toxicity and low biodegradability of commonly used second
24 generation ILs.^{13,14} Due to the above mentioned disadvantages,
25 over the last decade significant attention has been focused on
26 the development of novel ILs with enhanced green properties.
27 Recently, a third generation of ILs is emerging with structures
28 comprising of biodegradable and readily available nontoxic
29 ions such as natural bases, amino acids, sugars and naturally
30 occurring carboxylic acids.¹⁵⁻¹⁸

31 Together with this third generation ILs, deep-
32 eutectic-solvents (DES) formed by mixture of bio-based, non-
33 toxic, biodegradable and inexpensive salts (e.g. choline
34 chloride and urea or glycerol), represent also a promising
35 alternative option for using biodegradable ionic solvents in
36 biocatalysis and biotransformations.¹⁹⁻²¹

37 A family of third generation biocompatible ionic
38 liquids that are based on hydroxyl ammonium cation and
39 formic acid anion was described.²²⁻²⁷ These ILs display
40 significant scientific interest due to their low cost of
41 preparation and simple synthesis and purification methods,
42 since they can be easily formed by the stoichiometric
43 combination of a Brønsted acid with a Brønsted base.^{22,28}
44 Furthermore, both cation and anion exhibit a considerably low

45 toxicity and are biodegradable.^{14,18,29} For instance, formic acid
46 (methanoic acid), the simplest carboxylic acid that occurs
47 widely in nature and degrades readily in the presence of
48 oxygen, has low toxicity, hence it is used as a food additive and
49 as a preservative and antibacterial agent in livestock feed.^{29,30}
50 Moreover, the presence of hydroxyl groups significantly
51 decreases the toxicity (up to 100 times lower compared to
52 imidazolium- or pyridinium- based ILs) and improves the
53 biodegradability of quaternary ammonium cations^{14,31} leading
54 to ionic solvents that are biodegradable, recyclable and not
55 harmful to the environment compared to conventional
56 solvents.¹⁸

57 In this work, four hydroxyl ammonium based ILs,
58 formed by different cations and the same anion (formic acid)
59 such as: 2-hydroxyl ethylammonium formate (HEAF), 2-
60 hydroxy-*N*-methylethanaminium formate (HMEAF), 2-
61 hydroxy-*N,N*-dimethylethanaminium formate (HDMEAF) and
62 bis(2-hydroxyethyl) ammonium formate (BHEAF), were used
63 as media for oxidoreductions catalyzed by various biocatalysts
64 such as cytochrome c (cyt c), peroxidase, tyrosinase, laccase
65 and alcohol dehydrogenase. The structures of the ILs used in
66 the present work are depicted in Fig.1. Our interest for these
67 solvents arises from the fact that these hydroxyl ammonium-
68 based ILs have been labeled as biodegradable, recyclable and
69 environmentally friendly media.¹⁸ Although the effect of
70 different second generation ionic liquids formed with synthetic
71 anions on the catalytic behaviour of cyt c has been recently
72 described³², to our knowledge, there is no published study
73 regarding the catalytic behaviour of biocatalysts, including
74 metalloproteins, in third generation environmentally friendly
75 ILs, as those described in the present work. Therefore, a
76 detailed investigation of the effect of such ILs on the catalytic
77 and structural behaviour of biocatalysts is of great interest. In
78 the present work,, this effect on the biochemical and structural
79 characteristics of metalloproteins was investigated using cyt c
80 as a model protein, since it is one of the most thoroughly
81 physicochemically characterized metalloproteins^{33,34} with
82 biotechnological interest.³³⁻³⁵ Cyt c is a hemoprotein that could
83 catalyse peroxidase-like reactions in the presence of an electron
84 acceptor such as hydrogen peroxide (H₂O₂). In this catalytic
85 cycle, the reaction follows a ping pong mechanism. Firstly,
86 hydrogen peroxide reacts with cyt c to yield an intermediate
87 called Compound I. Reduction of Compound I leads to the

88 formation of Compound II, while the reducing substrate is
89 oxidized to the radical product. The reaction cycle is completed
90 by the second reduction step, in which Compound II oxidizes
91 another molecule of the reducing substrate.³⁶ Through kinetic
92 and stability studies, as well as the application of UV-vis,
93 ATR-FTIR and circular dichroism spectroscopic techniques,
94 we have investigated the effect of these neoteric ionic solvents
95 on the catalytic behaviour and structure of cyt c. Moreover, in
96 order to estimate the environmental impact of the above
97 mentioned ILs, their biodegradability has been assessed by
98 measuring the Biochemical Oxygen Demand (BOD).

99

100 Experimental Section

101 Materials

102 2-(methylamino) ethanol (Alfa Aesar), 2-(dimethylamino)-
103 ethanol (Alfa Aesar), diethanolamine (Merck), ethanolamine
104 (Sigma Aldrich), ethanol absolute (Sigma Aldrich) and formic
105 acid (Merck) were of the highest purity available (>99%) and
106 were used without further purification. Cytochrome c from
107 equine heart (>95% protein content), 552 U/mg solid (1 Unit
108 corresponds to the amount of enzyme that causes an increase in
109 absorbance at 470nm of 0.01 per minute at pH 7.0 and 25 °C in
110 a reaction mixture containing guaiacol and hydrogen peroxide),
111 peroxidase from horseradish HRP (E.C. 1.11.1.7.) ~ 66 %
112 protein content, 261 U/mg solid (1 Unit corresponds to the
113 amount of enzyme which produces 1mg of purpurogallin from
114 pyrogallol in 20 s at pH 6.0 at 25 °C) (type VI), tyrosinase from
115 mushroom *Agaricus bisporus* (EC 1.14.18.1), ~ 22 % protein
116 content, 3933U/mg solid (1 U unit corresponds to the amount
117 of enzyme that causes an increase in absorbance at 280nm of
118 0.001 per minute at pH 6.5 at 25 °C in a 3 ml reaction mixture
119 containing L-tyrosine), laccase from *Trametes versicolor* (E.C.
120 1.10.3.2), ~ 8.5 % protein content, 10 U/mg solid (1 Unit
121 corresponds to the amount of enzyme which converts 1 μmol
122 catechol per minute at pH 4.5 and 25 °C) and alcohol
123 dehydrogenase ADH from baker's yeast (E.C. 1.1.1.1), >90%
124 protein content, 440 U/mg solid (1 U converts 1.0 μmole of
125 ethanol to acetaldehyde per min at pH 8.8 at 25 °C) were
126 purchased from Sigma Aldrich and were used without further
127 purification. 2-methoxyphenol (guaiacol), 4-methyl-catechol
128 (>95%) and β-nicotinamide adenine dinucleotide (β-NAD⁺)

129 ($\geq 99\%$) were obtained from Sigma. 2,2'-azino-bis(3-
130 ethylbenzothiazoline-6-sulfonic acid) diammonium salt
131 (ABTS) and hydrogen peroxide (30% w/v) were purchased
132 from AppliChem and Fluka, respectively. H_2O_2 concentration
133 was determined spectrophotometrically at 240 nm ($\epsilon_{240}=43.6$
134 $\text{M}^{-1} \text{cm}^{-1}$).³⁷

135 136 Methods

137 138 Synthesis of ILs

139 Hydroxyl ammonium ILs were prepared by
140 neutralization of formic acid with different amines as described
141 in literature.¹⁸ 0.1 mol of amine compounds (2-(methylamino)-
142 ethanol, 2-(dimethylamino)-ethanol, diethanolamine and
143 ethanolamine) were placed in a two necked round-bottomed
144 flask equipped with a reflux condenser and a dropping funnel.
145 The flask was mounted in an ice bath due to the highly
146 exothermic nature of the acid-base reaction. Increased heat
147 could lead to dehydration of the salt to the corresponding
148 amide. The formic acid (0.1 mol) was added drop wise to the
149 flask under nitrogen atmosphere and vigorous stirring with a
150 magnetic stirrer. Stirring was continued for 24 hours at room
151 temperature in order to obtain a viscous clear liquid. ILs were
152 dried at high vacuum at 40 °C with continuous stirring to
153 remove the water content until no further weight loss was
154 detected. The reaction yields for the synthesis of all ILs studied
155 were more than 97%. The ionic liquids, when not in use, were
156 stored at room temperature in well-sealed glass vessels in a
157 desiccator.

158 The densities of all ILs at 20°C were measured by a
159 SVM 3000 Stabinger Viscometer (Anton Paar).

160 The chemical structure of the synthesized ILs was
161 determined by $^1\text{H-NMR}$, $^{13}\text{C-NMR}$, FT-IR and MS
162 spectroscopy. $^1\text{H-NMR}$ spectra (300MHz) and $^{13}\text{C-NMR}$
163 spectra (75MHz) were recorded on a Varian Gemini 2000 (300
164 MHz) spectrometer. ILs were dissolved in DMSO and CDCl_3 .
165 J values are given in Hz.

166 FT-IR (ATR method) spectra were recorded by a
167 JASCO 4200 spectrometer.

168 MS analysis was performed on a Varian 500 MS ion
169 trap mass spectrometer. Instrumental control and the data
170 processing were performed by the Varian MS workstation
171 software. The ionization type used was electrospray ionization.

172 Capillary voltage was 23.0 Volts. Analysis was conducted only
173 on the positive (ESI+) mode because the instruments cut-off
174 mass value is 50 and in the case of ILs studied, the HCOO^- ion
175 should appear at m/z 45.

176 *2-hydroxy-N-methylethanaminium formate* (HMEAF): δ_{H}
177 (300MHz; CDCl_3) 2.66 (3 H, s, CH_3^-), 3.03 (2 H, t, J 2.7, $-\text{O}-$
178 CH_2), 3.86 (2 H, t, J 3.0, $-\text{CH}_2-\text{N}$), 7.98 (3 H, br s, $-\text{NH}_2^+$ &
179 OH), 8.55 (1 H, s, H-COO).

180 δ_{C} (75 MHz, CDCl_3): 32.67, 50, 79, 56.74, 166.74.

181 FT-IR (ATR) $\nu_{\text{max}}/\text{cm}^{-1}$: 1340 ν (CN), 1469 ν_{sym} (COO^-), 1587
182 ν_{asym} (COO^-) & $\delta(\text{NH}_2^+)$, 2775 ν (NH_2^+), 3646 ν (OH).

183 MS (ESI): ES^+ m/z : 76.1 ($\text{OHCH}_2\text{CH}_2\text{NH}_2^+\text{CH}_3$, 100%)

184 Density (20°C): 1.1372 g/cm^3

185 *2-hydroxy-N,N-dimethylethanaminium formate* (HDMEAF): δ_{H}
186 (300MHz; CDCl_3) 2.74 (6 H, s, CH_3^-), 3.03 (2 H, t, J 6.0, $-\text{O}-$
187 CH_2), 3.87 (2 H, t, J 5.0, $-\text{CH}_2-\text{N}$), 8.58 (2 H, s, $-\text{NH}^+$ & OH),
188 9.48 (1H, s, H-COO).

189 δ_{C} (75 MHz, CDCl_3): 43.52, 56.42, 60.46, 168.99.

190 FT-IR (ATR) $\nu_{\text{max}}/\text{cm}^{-1}$: 1340 ν (CN), 1475 ν_{sym} (COO^-), 1600
191 ν_{asym} (COO^-), 2775 ν (NH^+), 3632 ν (OH).

192 MS (ESI): ES^+ m/z : 90.1 ($\text{OHCH}_2\text{CH}_2\text{NH}_2^+(\text{CH}_3)_2$, 100%)

193 Density (20°C): 1.0937 g/cm^3

194 *bis(2-hydroxyethyl)ammonium formate* (BHEAF): δ_{H}
195 (300MHz; DMSO) 2.87 (4 H, t, $-\text{O}-\text{CH}_2$), 3.59 (4 H, t, $-\text{CH}_2-$
196 N), 6.03 (4 H, br s, $-\text{NH}_2^+$ & OH), 8.34 (1 H, s, H-COO).

197 δ_{C} (75 MHz, CDCl_3): 49.70, 57.38, 166.61.

198 FT-IR (ATR) $\nu_{\text{max}}/\text{cm}^{-1}$: 1342 ν (CN), 1450 ν_{sym} (COO^-), 1587
199 ν_{asym} (COO^-) & $\delta(\text{NH}_2^+)$, 2798 ν (NH_2^+), 3658 ν (OH).

200 MS (ESI): ES^+ m/z : 106.2 ($\text{OHCH}_2\text{CH}_2)_2\text{NH}_2^+$, 100 %)

201 Density (20°C): 1.1587 g/cm^3

202 *2-hydroxyethylammonium formate* (HEAF): δ_{H} (300MHz;
203 DMSO- d_6): 2.81 (2 H, t, J 5.2, $-\text{O}-\text{CH}_2$), 3.56 (2 H, t, J 5.2, $-\text{O}-$
204 CH_2-N), 7.41 (4 H, br s, $-\text{NH}_3^+$ & OH), 8.41 (1 H, s, H-COO).

205 δ_{C} (75 MHz, CDCl_3): 49.70, 57.38, 166.61.

206 FT-IR (ATR) $\nu_{\text{max}}/\text{cm}^{-1}$: 1338 ν (CN), 1400 ν_{sym} (COO^-),
207 $\delta(\text{NH}_2^+)$, 1535 ν_{asym} (COO^-) & $\delta(\text{NH}_3^+)$, 2931-2863 ν (N^+H_3),
208 3623 ν (OH).

209 MS (ESI): ES^+ m/z : 62.0 ($\text{OHCH}_2\text{CH}_2)_2\text{NH}_3^+$, 100%)

210 Density (20°C): 1.2059 g/cm^3

211

212 Oxidation activity of metalloproteins

213 The peroxidase activity of cyt c and HRP was
214 determined by following the color formation during guaiacol
215 oxidation in the presence of H₂O₂. Reaction temperature was
216 set at 30 °C and the increase of the absorbance at 470 nm was
217 monitored at an interval of 2 seconds for a time period of 30
218 seconds as described elsewhere.³³ Reaction conditions were
219 adjusted according to the type of enzyme used for guaiacol
220 oxidation. In the case of cyt c, the oxidation reaction was
221 carried out in 50 mM sodium phosphate buffer pH 7.0 with 2
222 mM guaiacol, 20 mM of H₂O₂ and 13.8 U/mL of protein.³⁸ The
223 concentration of ILs in the reaction medium ranged between 0-
224 75% (v/v). When HRP (0.026 U/mL, 50 mM sodium phosphate
225 buffer pH 6.5) was used as a catalyst, the concentration of the
226 substrate was 20 mM and the concentration of H₂O₂ was 0.2
227 mM.³⁹

228 In the case of tyrosinase, 4-methyl catechol was used
229 as a substrate and quinone formation was monitored at 390 nm.
230 The reaction was started by adding 23.6 U/mL of tyrosinase
231 solution prepared in 50 mM phosphate buffer pH 6.8,
232 containing 10 mM of the substrate at 27 °C.

233 Laccase activity was evaluated using ABTS as a
234 substrate. Reaction mixture contained 1 mM ABTS and 0.0084
235 U/mL enzyme in 100 mM acetate buffer pH 4.6 at 27 °C and
236 the absorbance change was measured at 415 nm.⁴⁰ For all
237 enzymatic oxidations, the amount of oxygen has been
238 considered in excess, since the reaction mixture was vortexed
239 for saturation with oxygen before adding the enzyme solution.

240 Activity of ADH was determined by measuring the
241 rate of reduction of β-NAD⁺ by ethanol at 340 nm. 10 U/mL
242 stock solution of enzyme was prepared immediately prior to
243 the reaction in 10 mM sodium phosphate buffer pH 7.5. In a
244 typical reaction mixture, 5 mM β-NAD⁺ and ethanol (3.2%,
245 v/v) were added in 50 mM sodium phosphate buffer pH 8.0.
246 The enzymatic reaction was initiated with the addition of 8 μL
247 of ADH solution (0.08 U/mL) to the reaction mixture at 25 °C.
248 The increase in absorbance due to β-NADH formation was
249 monitored at 340 nm.⁴¹

250 In all cases studied, the reaction mixture (1mL) was
251 homogeneous and no precipitation was observed in the
252 presence of all ILs. Moreover, after incubation of ILs with
253 H₂O₂, no modification of their structure was observed by NMR
254 analysis in all cases studied. In order to avoid the ionic liquids-
255 induced interference to the pH, all the reaction media (buffer-

256 ionic liquids solutions) were re-adjusted (with HCl or NaOH)
257 to the required pH before being used in the biocatalytic
258 reactions. All reactions were performed at the optimal pH
259 required in each case. All experiments were performed in
260 triplicate. Control experiments without biocatalyst were also
261 carried out and no conversion of the substrates was observed in
262 all cases studied. All the reaction rates were calculated from
263 the slope of the linear portion of plots of absorbance versus
264 time. The relative activity was expressed in each case as the
265 ratio of activity in the presence of ILs to that observed in buffer
266 solutions.

268 Kinetic study of cyt c and activation energy (E_a) 269 determination

270 Guaiacol oxidation in the presence of H₂O₂ at 30 °C
271 was used as a model reaction for the determination of the effect
272 of various ILs on the kinetic constants of cyt c.³⁶ In a typical
273 experimental procedure, guaiacol was added to a final
274 concentration of 2 mM, while H₂O₂ concentration was in the
275 range of 0.05-100 mM. The concentration of cyt c used in the
276 reaction was 25 μg/mL. The oxidation of guaiacol was
277 monitored at 470 nm and the extinction coefficient for the
278 oxidation product was considered equal to ε= 26.6 mM⁻¹ cm⁻¹
279 in all cases studied.⁴² The apparent kinetic parameters of
280 maximum velocity V_{max}^{app} and Michaelis-Menten constant
281 K_m^{app} were determined through Michaelis-Menten equation for
282 initial reaction velocity. All the kinetic parameters were
283 determined by non-linear regression analysis using the program
284 Enzfitter (Biosoft, Cambridge, UK). Data reported are the
285 mean values of three independent experiments. For the
286 determination of the activation energy E_a for the oxidation of
287 guaiacol catalyzed by cyt c, reactions were performed in 1 mL
288 co-solvent mixtures of 50 mM sodium phosphate buffer pH 7.0
289 and 30% (v/v) aqueous solutions of ILs containing 2 mM
290 guaiacol, 100 mM H₂O₂ and 25 μg/mL of cyt c at a temperature
291 range from 20 to 60 °C. The activation energy E_a was
292 calculated from the Arrhenius plot through linear regression
293 analysis.

294 Stability study of cyt c

295 Stability study of cyt c was performed by incubating
296 cyt c (13.8 U/mL) in aqueous solutions of ILs containing 1 mM

297 H₂O₂ at 30 °C. The incubation mixture did not contain guaiacol
298 since the presence of reducing substrates in the reaction
299 mixture could increase the stability of cyt c against H₂O₂.^{43,44}
300 After 15 min of incubation, 200 µL of sample were removed
301 and transferred to a 96-well microplate in order to determine
302 the remaining peroxidase activity of cyt c using guaiacol (2
303 mM) as a substrate, as described before. All experiments were
304 performed in triplicate.

305 UV-vis spectroscopy

306 A double-beam UV-vis spectrophotometer (UV-1601
307 Shimadzu, Tokyo, Japan) was used in order to monitor the
308 effect of aqueous solutions of ILs on the absorption spectrum
309 of cyt c (25 µg/mL) in a standard 1 cm path length quartz
310 cuvette. UV-vis absorption spectra of cyt c was recorded at 30
311 °C.

312 ATR-IR Spectroscopy

313 Single pass attenuated total reflection Fourier
314 transform infrared (ATR-FTIR) spectra were recorded on a
315 Shimadzu FT-IR 8400 (Tokyo, Japan) infrared
316 spectrophotometer equipped with a deuterated triglycine sulfate
317 (DTGS) detector in the region of 400- 4000 cm⁻¹ using a
318 (ZnSe)-attenuated total reflection accessory. 200 scans were
319 collected for each sample at 2 cm⁻¹ resolution and 1 cm⁻¹ time
320 interval. The concentration of cyt c was 5 mg/mL in buffer and
321 9 mg/mL in 30% (v/v) aqueous solutions of ILs. Reference
322 spectra under identical conditions without the presence of cyt c
323 were also recorded. Data analysis of the Amide I region and
324 band assignment were performed as described elsewhere.⁴⁵

325 Circular Dichroism Spectroscopy

326 Soret region CD spectra (350-450 nm) of cyt c (200
327 µg/mL) in 0.5 mM sodium phosphate buffer pH 7.0 and in 60%
328 (v/v) aqueous solution of ILs were obtained using a Jasco J-815
329 spectropolarimeter (Tokyo, Japan) in a 1 cm path length quartz
330 cell. All spectra were obtained at 25 °C with a 2 nm bandwidth
331 and a scan speed of 10 nm/min. For every medium scanned, a
332 baseline was recorded and subtracted from the protein
333 spectrum. All scan measurements were performed in triplicate.

334 Dye decolorization

335 The decolorization activity of cyt c was measured by
336 following color elimination of pinacyanol chloride (1,1'-
337 diethyl-2,2'-carbocyanine chloride) with H₂O₂ in buffer and in
338 the presence of various amounts of ILs. The reaction mixture
339 contained 130 µM pinacyanol chloride and 80 µg/mL cyt c.
340 The oxidation of the dye was started by adding 0.3 mM H₂O₂
341 at 27 °C under stirring at 300 rpm. At predetermined time
342 intervals 30 µL aliquots were removed from the reaction
343 mixture and added to a 1:1 (v/v) mixture of methanol and 50
344 mM sodium phosphate buffer pH 7.0. The remaining
345 concentration of the dye was monitored by measuring the
346 absorbance at 603 nm using an extinction coefficient for
347 pinacyanol chloride equal to $\epsilon = 82,350 \text{ M}^{-1} \text{ cm}^{-1}$.⁴⁶

348 Recycle of ILs

349 The enzymatic decolorization of pinacyanol chloride
350 was further used in order to investigate the reusability of the
351 ILs. In this case, cyt c was immobilized on celite in a similar
352 manner as described elsewhere⁴⁷, in order to facilitate the
353 recovery of the enzyme and the reuse of ILs. The reaction
354 mixture (0.5ml) contained 130 µM pinacyanol chloride and 30
355 mg/mL of immobilized biocatalyst (containing 2 µg of cyt c
356 per 1 mg of celite). The oxidation of the dye was started by
357 adding 0.3 mM H₂O₂. The reaction mixture was incubated at
358 27 °C under stirring at 300 rpm for 3 hours. At the end of the
359 incubation, 1 ml of water was added to the reaction mixture
360 and the immobilized biocatalyst was filtered off. The aqueous
361 filtrate containing the ILs was washed with ethyl acetate in
362 order to remove any amount of the residual substrates and
363 products and then the water was evaporated in vacuo. The
364 residual IL was dried under high vacuum at 40 °C until
365 constant weight. The structure and purity of the recycled IL
366 were verified with ¹H-NMR, while the recycle process was
367 repeated up to three times.

368 Biodegradability test

369 The biodegradability of four ILs has been assessed
370 by measuring the Biochemical Oxygen Demand (BOD).^{18,48}
371 Biodegradation tests were carried out according to the
372 manometric respirometric method to determine the oxygen
373 demand for the biochemical degradation of each organic
374 substance after five days. A detailed description of the method
375 is described on the Supplementary data.

376

377 Results and Discussion

378 Effect of hydroxyl ammonium ILs on the activity of various 379 metalloproteins.

380 In the present study, the effect of four hydroxyl
381 ammonium-based ILs (HEAF, HMEAF, HDMEAF and
382 BHEAF) on the activity of various metalloproteins such as
383 cytochrome c from horse heart (cyt c), horse radish peroxidase
384 (HRP), mushroom tyrosinase, laccase from *Trametes versicolor*
385 and alcohol dehydrogenase (ADH) from baker's yeast was
386 investigated (Table 1). In most cases studied, the presence of
387 5% (v/v) hydroxyl ammonium ILs in the reaction medium
388 affected the activity of metalloproteins. The effect of ILs used
389 on the enzymatic activity depended on the biocatalyst used, as
390 well as on the nature of the cation of IL used. Particularly in
391 the case of HRP and ADH, the activity remained unchanged or
392 decreased, depending on the IL used. The oxidation activity of
393 laccase was significantly reduced in all ILs tested, which is in
394 accordance to that reported for imidazolium-based water
395 miscible ILs.⁴⁹ However, it must be pointed out that, in the case
396 of cyt c, the presence of hydroxyl ammonium ILs in the
397 reaction medium significantly enhanced (up to 3.4 fold) its
398 peroxidation activity. An enhanced activity was also observed
399 for tyrosinase in the presence of HMEAF and BHEAF IL.

400

401 Effect of ILs on the peroxidative activity of cyt c

402

403 In order to further investigate the effect of hydroxyl
404 ammonium-based ILs on the catalytic behaviour of
405 metalloproteins, cyt c was chosen as a model protein. The
406 effect of the concentration of various hydroxyl ammonium ILs
407 on the peroxidase activity of cyt c using guaiacol as a substrate
408 is shown in Fig. 2. As it can be seen, the peroxidase activity of
409 cyt c strongly depends on the nature of cations and the
410 concentration of ILs used, which is in accordance to that
411 observed previously for imidazolium, alkyl ammonium and
412 choline-based ILs^{42, 50-52}. In most cases, the increase of the ILs
413 concentration significantly increases the peroxidase activity of
414 cyt c. A 9-fold and 20-fold activity enhancement was observed
415 respectively in BHEAF and HEAF at a concentration of ILs
416 equal to 60% (v/v), compared to buffer. Similar catalytic

417 activation of cyt c in the presence of these ILs was observed for
418 ABTS oxidation (data not shown), indicating that this
419 activation effect is independent of the substrate used. Although
420 cyt c activity has been studied in other biocompatible ILs, such
421 as alkyl ammonium and choline-based ILs, in those cases no
422 activation was observed, in contrast to the results obtained in
423 our study.^{50,52} It is interesting to note that, when equimolar
424 amounts of individual components of these ionic liquids
425 (hydroxyl amines and formic acid) were both added in buffer
426 solution (the amounts of the individual components
427 corresponded to the ones present in ILs and were adjusted
428 according to the desired concentration of ILs in buffer), no or
429 low catalytic activity of cyt c was observed (Fig.S.17.
430 Supplementary). This clearly indicates that, the beneficial
431 effect of ILs on the catalytic activity of cyt c is associated to
432 the formed salt and not to their individual components.

433 In order to gain a deeper insight into the influence of
434 the hydroxyl ammonium-based ILs on the peroxidase activity
435 of cyt c, the effect of the ILs on the apparent kinetic constants
436 V_{\max}^{app} and K_m^{app} of cyt c for the oxidation of guaiacol with
437 H_2O_2 were determined. The effect of the nature and
438 concentration of ionic liquids on the catalytic efficiency,
439 expressed by the ratio $V_{\max}^{\text{app}}/K_m^{\text{app}}$ (in all cases studied the cyt
440 c concentration was the same), is presented in Fig. 3. As it can
441 be seen, the presence of ILs enhances, in most cases, the
442 catalytic efficiency of cyt c compared to buffer solution. The
443 highest catalytic efficiency was observed when HEAF was
444 used as co-solvent, causing a more than 20-fold increase in
445 catalytic efficiency at a concentration of this IL higher than
446 60% (v/v). The increased catalytic efficiency observed at high
447 concentrations of HEAF and BHEAF was the result of a
448 simultaneous increase of V_{\max}^{app} and decrease of K_m^{app}
449 compared to that observed in buffer (Table S1). The low
450 apparent K_m^{app} values observed at high concentrations of
451 HEAF and BHEAF indicate that the affinity of cyt c towards
452 the substrate was increased, which may be correlated with
453 structural changes in the active site of cyt c and therefore,
454 changes in the microenvironment of heme.^{38,53} The increased
455 catalytic efficiency observed here is in accordance to that
456 reported for various enzymes in other ionic liquid-based
457 systems.⁵³⁻⁵⁶ It was suggested that, the presence of ILs in the
458 reaction medium can increase the affinity of the enzyme to the
459 substrate, resulting in a higher catalytic efficiency compared to

460 other media, such as organic solvents and aqueous
461 solutions.^{55,56}

462 It has been proposed by several researchers that the
463 enzyme performance in hydrophilic ILs could be affected by
464 the kosmotropicity/chaotropicity properties of the ions of
465 ILs.⁵⁷⁻⁵⁹ Ions that are considered as kosmotropes promote water
466 structure, while chaotrope ones can suppress it.⁶⁰ In the present
467 study, formic acid, used as the anion for the formation of all
468 ILs tested, is considered as a kosmotropic anion.⁶¹ On the other
469 hand, hydroxyl alkyl ammonium cations, which are more
470 hydrophilic than the chaotropic choline cation, could be
471 assumed to be highly chaotropic.⁴³ This indicates that, the
472 presence of a kosmotropic anion and a chaotropic cation
473 improved the catalytic efficiency of cyt c which is in
474 accordance to that proposed for other enzymes in different
475 ionic liquids.⁵⁷⁻⁵⁹ It seems that, there is a correlation between
476 the chaotropicity of the cation and the catalytic efficiency of
477 cyt c in these media. More specifically, in the case of more
478 hydrophilic and thus more chaotropic BHEAF and HEAF
479 cations, the catalytic efficiency of cyt c was higher compared
480 to that observed for less chaotropic HMEAF and HDMEAF.

481 In order to further investigate the effect of these ILs
482 on the peroxidase catalytic behavior of cyt c, the activation
483 energy (E_a) of cyt c for the oxidation of guaiacol in buffer, as
484 well as in the presence of 30% (v/v) aqueous solutions of
485 hydroxyl ammonium IIs, was determined over a temperature
486 range of 20 to 60 °C. The activation energies in various media,
487 calculated from the slope of the Arrhenius plots, are presented
488 in Table 2. As it can be seen, the presence of ILs in the reaction
489 mixture decreases the activation energy compared to that in
490 buffer solution and this decrease is more pronounced when
491 HMEAF and HEAF are used. This decrease in E_a value
492 observed here may be correlated to the effect of ILs on the
493 structure of the protein molecule and the formation of enzyme-
494 substrate complex, as it was proposed for imidazolium-based
495 ionic liquids.⁵⁶

497 **Stability of cyt c against H₂O₂ in ILs**

498 It is well known that, heme-containing enzymes,
499 such as peroxidases and cyt c, are inactivated by H₂O₂ in the
500 absence of reducing substrate in aqueous media.^{43,62} This
501 inactivation may be correlated to the modification of heme
502 resulting in the formation of a verdohemoprotein, an inactive

503 form of heme, as a final product, as well as in the formation of
504 radical species that could react and inactivate the heme
505 center.⁶⁰⁻⁶⁵

506 In order to investigate the stability of cyt c against
507 H₂O₂ in hydroxyl ammonium-based ILs, cyt c was incubated in
508 the presence of 1 mM H₂O₂ for 15 min at 30 °C in buffer
509 containing various ILs (30-60% v/v) and the remaining
510 peroxidase activity was determined using guaiacol as a
511 reducing substrate (Fig. 4).

512 As seen in Fig. 4, the peroxidase activity of cyt c in
513 buffer was reduced by 40% after incubation with H₂O₂. The
514 tolerance of cyt c, in the presence of all ILs used, strongly
515 depends on the nature of ILs cations, while the effect of their
516 concentration is not so obvious. Namely, in the presence of
517 HMEAF and especially HDMEAF, the remaining activity of
518 cyt c in most cases was higher compared to that observed in
519 buffer, indicating that these ILs protect the protein from H₂O₂
520 deactivation. However, in the presence of HEAF or BHEAF,
521 the remaining peroxidase activity of cyt c after incubation with
522 H₂O₂ was significantly decreased compared to that observed in
523 buffer, for all concentrations tested.

524 It was reported that the stability of cyt c in the
525 presence of various hydrophilic ILs was strongly influenced by
526 the kosmotropicity/chaotropicity of the ions of ILs.⁵⁰ However,
527 in our study, the effect of ILs on stability of cyt c does not
528 follow the Hofmeister series and therefore, the chaotropicity of
529 their cations. It seems that kosmotropicity/chaotropicity is not
530 the only key in determining the cyt c behavior in ILs.

531 It is interesting to note that, all the ILs used in the
532 present work are formed by hydroxyl ammonium cations. As it
533 has been proposed, these cations can mimic the molecular
534 structure of water with H-bond accepting/donating
535 functionalities forming hydrogen bonds with the polypeptide
536 backbone of protein and thus affecting its structure and
537 function.⁵⁹ It is worth noting that, these interactions should not
538 be too strong in order to avoid the dissociation of the hydrogen
539 bonds between the amino acids which could lead to the
540 disruption of the protein structure.⁶⁶ Based on the basicity of
541 nitrogen of the amine residues of the ILs studied, the H-
542 bonding capability should increase by the following order:
543 HDMEAF < HMEAF < HEAF < BHEAF.⁶⁷ As it can be seen in
544 Fig. 3, cyt c is more stable in aqueous solutions of HDMEAF
545 and HMEAF ILs, which could be possibly explained by the

546 decreased H-bond ability and thus reduced interaction of these
547 ILs with the protein molecule.

548 Moreover, the increased stability of cyt c against
549 H₂O₂ in HDMEAF could be attributed to the less hydrophilic
550 environment surrounding the protein created by this IL. The
551 less hydrophilic environment created by HDMEAF could limit
552 the diffusion of hydrophilic H₂O₂ towards the protein
553 microenvironment, thus reducing its denaturing effect. The
554 possible limited diffusion of H₂O₂ to the microenvironment and
555 thus to the active center of cyt c could probably also explain
556 the decreased activity of cyt c observed in HDMEAF-based
557 reaction medium (Fig. 3).

558 Structural characterization of cyt c using spectroscopic 559 techniques.

561 The effect of the hydroxyl ammonium ILs on the
562 conformation of cyt c was investigated through ATR-FTIR,
563 UV-Vis and circular dichroism (CD) spectroscopy. The
564 conformational changes of cyt c in the presence of hydroxyl
565 ammonium ILs-based media compared to its structure in buffer
566 (50 mM sodium phosphate, pH 7.0) were investigated by ATR-
567 FTIR spectroscopy. The analysis of the Amide I band at
568 approximately 1600–1700 cm⁻¹ (mainly due to the C=O
569 stretching vibration) makes it possible to obtain information on
570 the effect of ILs on the secondary structure of the protein.⁶⁸⁻⁷¹

571 Correlation coefficients (r) between the Amide I
572 spectra of cyt c dissolved in buffer and 30% (v/v) aqueous
573 solutions of ILs were evaluated according to previous studies.⁷¹
574 In particular, the correlation coefficient was calculated using
575 the formula

$$576 \quad r = \frac{\sum x_i y_i}{\sqrt{\sum x_i^2 \sum y_i^2}},^{54}$$

577 where *x* and *y* are the absorbance values of the cyt c spectrum
578 dissolved in buffer and 30% (v/v) of ILs respectively, at the *i*th
579 frequency position for the range 1600-1700 cm⁻¹ (Amide I).
580 For identical spectra, a value of 1.0 will be returned.⁷¹ Table 3
581 shows the correlation coefficients and the differences on α -
582 helix content of cyt c in the presence of various ILs-based
583 media compared to buffer, as a result of ATR-FTIR analysis.
584 As it can be seen in Table 3, the relative structure of cyt c in
585 the presence of all ILs used is close to that in buffer. Similar
586 retention of the secondary structure of cyt c in various media

588 composed by other hydrophilic ILs has also been previously
589 reported.^{50,51}

590 Since the most abundant element (about 40%) of the
591 secondary structure of cyt c is α -helix,⁷² we also determined the
592 effect of ILs on α -helix content (Table 3). The α -helix content
593 was identified from the second-derivative ATR-FTIR spectra
594 of the protein in various media, taking into consideration that
595 the bands at 1650–1660 cm⁻¹ were assigned to α -helix.^{73,74} As it
596 can be seen, a slight increase in α -helix content was observed
597 in aqueous solutions of HMEAF, HDMEAF and HEAF that
598 can be correlated to a more rigid structure of the protein.⁷⁵ On
599 the other hand, the decrease in α -helix content observed in
600 BHEAF-based media could be attributed to a less rigid
601 structure of cyt c that could be correlated to the substantially
602 low stability of the protein observed in this IL (Fig. 4).

603 Conformational changes of the heme prosthetic
604 group of cyt c in aqueous solutions of hydroxyl ammonium
605 ILs-based media were further investigated using UV-Vis
606 spectroscopy. As it can be seen in Fig. 5 and Fig. 6, the
607 oxidized (Fe(III)) form of cyt c in buffer has a characteristic
608 UV-vis spectrum consisting of a sharp Soret band at 409 nm, a
609 weaker, broad Q-band at 530nm and a very weak charge
610 transfer band from the sulfur atom of Met80 (the axial ligand)
611 with heme Fe(III) observed at 695 nm, which is in accordance
612 to that reported by other researchers.⁷⁶⁻⁷⁷

613 The incubation of cyt c in 60% (v/v) aqueous
614 solutions of HDMEAF, BEHAF and HEAF did not affect the
615 UV-Vis spectrum of the protein (Fig.5) suggesting that the
616 polypeptide environment around the heme has been kept
617 intact.⁷⁸ However, the UV-vis spectrum of cyt c in 60% (v/v)
618 aqueous solution of HMEAF was significantly changed (Fig.
619 5). More specifically, the Soret band of the protein was moved
620 at 413 nm, while at Q-band region a sharp α -band at 550 nm
621 and a sharp β -band at 520 nm appeared, indicating cyt c in
622 reduced state.⁷⁹

623 Moreover, in HMEAF-based media, the charge
624 transfer band at 695 nm was significantly reduced compared to
625 that observed for the native protein (Fig. 6). This spectral
626 change indicates the partial perturbation or cleavage of the
627 coordination bond of Met80 with the heme iron.⁸⁰ The loss of
628 the heme's axial sulfur-coordinated ligand has been correlated
629 with the progressive breaking of hydrogen bonds in the protein
630 interior and gradual exposure of amino acid residues and the

631 porphyrin ring and hence loss of iron and the catalytic activity
632 of the protein.^{78,81}

633 The structural changes of cyt c observed in HMEAF-
634 based media were further investigated using CD spectroscopy.
635 Unfortunately, due to high absorbance of the IL in far and near
636 UV region, only the Soret region of the CD spectrum (350-450
637 nm) of cyt c could be investigated, which can provide further
638 insight on structural changes of the heme crevice.^{38,82,83} Fig. 7
639 shows the CD spectra of cyt c in 0.5 mM sodium phosphate
640 buffer pH 7.0 and in the presence of HMEAF (60% v/v). The
641 spectrum of cyt c, in its native conformation in buffer, exhibits
642 a negative peak at 416 nm and a positive peak at 402 nm, due
643 to a split Cotton effect.⁸³ As it can be seen in Fig. 7, the
644 addition of HMEAF increases the positive band at 402 nm and
645 significantly vanishes the negative band at 416 nm. Similar
646 spectral changes have been previously reported due to
647 interactions of cyt c with other ILs and organic
648 solvents,^{33,51,52,84,85} as well as with denaturants, such as
649 guanidine, HCl or urea.⁸⁶

650 The increase of the positive peak at 416 nm and the
651 disappearance of the negative peak at 402 nm observed here
652 could be attributed to the disordered orientation and
653 disturbance of the distance between the heme on the Met80
654 side and the aromatic residues Try-59 and Phe-82 in the
655 polypeptide backbone of the heme crevice.⁸⁷ Similar results
656 have also been observed when cyt c was dissolved in hydrated
657 pyridinium-based and neat imidazolium based ILs.^{51,85} The
658 findings from circular dichroism studies correlate well with the
659 UV-vis data described before, as well as with the reduced
660 peroxidase activity of cyt c in the presence of HMEAF
661 compared to the other ILs used in the present work (Fig. 3, 5,
662 6).

664 **Decolorization of pinacyanol chloride by cyt c in ILs-based** 665 **media**

666 The accumulation of industrial dyes in wastewater
667 has a profound environmental and health impact and, therefore,
668 their removal is a substantial challenge for the scientific and
669 industrial community.⁸⁸ Several oxidative biocatalysts have
670 been used for the enzymatic elimination of dyes including cyt
671 c, laccases, peroxidases, etc.^{44,89-92} In order to investigate the
672 effect of the hydroxyl-ammonium ILs on the decolorization
673 activity of cyt c, we used pinacyanol chloride as a model

674 substrate, which is a symmetric trimethinecyanine dye with
675 industrial use.⁹³ In this case, the initial concentration of H₂O₂
676 was kept low (0.3mM) in order to reduce its denaturing effect.
677 As it can be seen in Fig. 8 and Table 4, the decolorization
678 activity of cyt c, in the presence of all ILs studied, strongly
679 depends on the nature of the cation used, as well as the
680 concentration of the ILs in the reaction media. In the case of
681 HMEAF, the decolorization efficiency decreased, while the use
682 of BHEAF and HEAF enhanced the ability of cyt c to
683 decolorize the dye compared to that observed in buffer. More
684 specifically, the decolorization rate in the presence of HEAF
685 and BHEAF in the reaction mixture was up to 4-fold and 5-fold
686 higher, respectively, compared to that in buffer. It is worth
687 noting that, the decolorization yield was about 90% after 20
688 min of incubation in media containing various concentrations
689 of HEAF and BHEAF (15-60% v/v), while in buffer the
690 decolorization yield was less than 40%. The positive effect of
691 these two ILs increases with the increase of their concentration
692 in the reaction mixture. The high decolorization activity of cyt
693 c in reaction media containing BHEAF or HEAF could be
694 attributed to the enhanced peroxidation activity of cyt c
695 observed in these media (Fig.3). In order to further demonstrate
696 the green properties of these novel ILs, their recyclability and
697 reusability were also investigated, using the catalyzed by cyt c
698 decolorization of pinacyanol chloride as a model reaction (see
699 Experimental section). All ILs were reused in the same
700 decolorization reaction up to three times with comparable
701 decolorization yields to those observed for the initial reaction.
702 The beneficial effect of hydroxyl ammonium-based ILs on the
703 decolorization activity of cyt c together with their reusability
704 indicate that these ILs could be considered as promising
705 environmentally friendly media for biocatalytic decolorization
706 of dyes.

707 **Biodegradability assessment of ILs**

708 In order to determine the biodegradability level of the
709 synthesized ILs, the biological oxygen demand (BOD) for the
710 biochemical degradation of each IL after five days was
711 determined. During the BOD test, the carbonaceous demand
712 (which refers to the conversion of organic carbon to carbon
713 dioxide) was taken into account and the results are reported as
714 carbonaceous BOD (CBOD).¹⁸ The results of the
715 biodegradation of the ILs are presented in Table 5.

716 The experimental results indicated that all ILs
 717 studied present remarkable biodegradability potential, since a
 718 percentage of more than 50% of the organic carbon was
 719 biodegraded within five days. The relatively high
 720 biodegradability of these ILs could be attributed to the
 721 presence of hydroxyl groups on the ILs cations. It has been
 722 reported that the biodegradability level of similar
 723 ethanalamine-based ILs depends mainly on the cation of the IL
 724 molecule and on the groups that provide possible sites for
 725 enzymatic hydrolysis, especially oxygen atoms (e.g. in the
 726 form of hydroxyls) that present high degradation potential.<sup>14,94-
 727 96</sup>

728 Conclusions

729 Herein, neoteric, low cost and biodegradable ILs,
 730 based on the combination of a hydroxyl ammonium cation
 731 and formic acid, have been prepared and used as media for
 732 biocatalytic oxidation catalyzed by metalloproteins.
 733 Kinetic and structural studies of cyt c indicate that the
 734 presence of these ILs in the reaction mixture has a
 735 considerable beneficial effect on the catalytic efficiency
 736 and tolerance against hydrogen peroxide, while the protein
 737 structure is slightly affected. The effect of these ILs on the
 738 catalytic behaviour of cyt c strongly depends on the
 739 structure of the hydroxyl ammonium cations used for their
 740 formation. Moreover, the beneficial effect of hydroxyl
 741 ammonium-based ILs on the biocatalyzed degradation of
 742 an industrial dye, together with their efficient recyclability
 743 and reusability, indicate the potential application of these
 744 novel ILs as green media for biotransformations of
 745 industrial interest. The use of immobilized enzymes^{97,98} or
 746 the use of ILs as a support for enzyme immobilization^{99,100}
 747 is expected to facilitate the recovery and reuse of both the
 748 biocatalyst and the ILs, enhancing therefore the green
 749 character of such biocatalytic processes. Further
 750 investigation on the effect of the nature and
 751 physicochemical properties of cations and anions used for
 752 the formation of such environmentally friendly ILs on the
 753 catalytic behaviour of various industrial enzymes is in
 754 progress in our lab.

755

756

757

758

759 Acknowledgements

760 This research project has been co-financed by the
 761 European Union (European Regional Development Fund-
 762 ERDF) and Greek national funds through the Operational
 763 Program "THESSALY- MAINLAND GREECE AND
 764 EPIRUS-2007-2013" of the National Strategic Reference
 765 Framework (NSRF 2007-2013). Also the support from
 766 bilateral Personnel Exchange Programme between Greece
 767 and Germany (IKYDA 2015) is acknowledged. The
 768 authors would like to thank the Atherothrombosis
 769 Research Centre of the University of Ioannina for
 770 providing access to the facilities.

771

772 Notes and references

773 ^a Department of Biological Applications and Technology,
 774 Laboratory of Biotechnology, University of Ioannina, University
 775 Campus, 45110 Ioannina, Greece

776 ^b School of Chemical Engineering, Laboratory of Organic
 777 Chemistry, National Technical University of Athens, Heroon
 778 Polytechniou 9, Zografou Campus, 15780 Athens, Greece

779 E-mail: hstamati@cc.uoi.gr (H. Stamatis)

780 URL: <http://biotechlab.bat.uoi.gr/index.php/en/>

781 Tel.: +30 26510 97116; fax: +30 26510 97343

782 Electronic Supplementary Information (ESI) available

783

784

785

786 1 P. Lozano, *Green Chem.*, 2010, **12**, 555.

787 2 J. Gorke, F. Srienc and R. Kazlauskas, *Biotechnol.*
 788 *Bioprocess Eng.*, 2010, **15**, 40–53.

789 3 H. Olivier-Bourbigou, L. Magna and D. Morvan,
 790 *Appl. Catal. A Gen.*, 2010, **373**, 1–56.

791 4 S.G. Cull, J. D. Holbrey, V. Vargas-Mora, K. R.
 792 Seddon, and G. J. Lye, 2000, *Biotechnol. Bioeng.* **69**,
 793 227-233.

794 5 S. Park and R. J. Kazlauskas, *Curr. Opin.*
 795 *Biotechnol.*, 2003, **14**, 432–437.

796 6 F. van Rantwijk and R. A Sheldon, *Chem. Rev.*,
 797 2007, **107**, 2757–2785.

798 7 T. Welton, *Chem. Rev.*, 1999, **99**, 2071-2083.

799 8 U. Kragl, M. Eckstein and N. Kaftzik, *Curr. Opin.*
 800 *Biotechnol.*, 2002, **13**, 565–71.

801 9 R. A. Sheldon, R. M. Lau, M. J. Sorgedraeger, F. van
 802 Rantwijk and K. R. Seddon, *Green Chem.*, 2002, **4**,
 803 147-151.

- 804 10 P. Domínguez de María, *Angew. Chem. Int. Ed. Engl.*, 2008, **47**, 6960–8.
805
- 806 11 M. H. Katsoura, A. C. Polydera, L. D. Tsironis, M. P. Petraki, S. K. Rajacić, A. D. Tselepis and H. Stamatis, *Biotechnol.*, 2009, **26**, 83–91.
807
808
- 809 12 A. A. Papadopoulou, M. H. Katsoura, A. Chatzikonstantinou, E. Kyriakou, A. C. Polydera, A. G. Tzakos and H. Stamatis, *Bioresour. Technol.*, 2013, **136**, 41–48.
810
811
812
- 813 13 M. Matzke, S. Stolte, K. Thiele, T. Juffernholz, J. Arning, J. Ranke, U. Welz-Biermann and B. Jastorff, *Green Chem.*, 2007, **9**, 1198–1207.
814
815
- 816 14 T. P. T. Pham, C.-W. Cho and Y.-S. Yun, *Water Res.*, 2010, **44**, 352–72.
817
- 818 15 K. Fukumoto, M. Yoshizawa and H. Ohno, *J. Am. Chem. Soc.*, 2005, **127**, 2398–9.
819
- 820 16 Z. Guo, B. Chen, R. López Murillo, T. Tan and X. Xu, *Org. Biomol. Chem.*, 2006, **4**, 2772–6.
821
- 822 17 J. Wang, T. L. Greaves, D. F. Kennedy, A. Weerawardena, G. Song and C. J. Drummond, *Aust. J. Chem.*, 2011, **64**, 180.
823
824
- 825 18 A. Tzani, A. Douka, A. Papadopoulos, E. A. Pavlatou, E. Voutsas and A. Detsi, *ACS Sustainable Chem. Eng.*, 2013, **1**, 1–6.
826
827
- 828 19 J. Gorke, F. Srienc and R. Kazlauskas, *Chem. Commun.*, 2008, **10**, 1237–1237.
829
- 830 20 E. Durand, J. Lacomte and P. Villeneuve, *Eur. J. Lipid Sci. Technol.*, 2013, **115**, 379–385.
831
- 832 21 P. Domínguez de María and Z. Maugeri, *Curr. Opin. Chem. Biol.*, 2011, **15**, 220–225.
833
- 834 22 N. Bicak, *J. Mol. Liq.*, 2005, **116**, 15–18.
- 835 23 X. L. Yuan, S. J. Zhang and X. M. Lu, *J. Chem. Eng. Data*, 2007, **52**, 596–599.
836
- 837 24 M. Iglesias, a. Torres, R. Gonzalez-Olmos and D. Salvatierra, *J. Chem. Thermodyn.*, 2008, **40**, 119–133.
838
839
- 840 25 M. Khodadadi-Moghaddam, A. Habibi-Yangjeh and M. R. Gholami, *J. Mol. Catal. A Chem.*, 2009, **306**, 11–16.
841
842
- 843 26 H. Choi and I. Kwon, *Ind. Eng. Chem. Res.*, 2011, **50**, 2452–2454.
844
- 845 27 M. Ismail Hossain, M. El-Harbawi, Y. A. Noaman, M. A. B. Bustam, N. B. M. Alitheen, N. A. Affandi, G. Hefter and C.-Y. Yin, *Chemosphere*, 2011, **84**, 101–104.
846
847
848
- 849 28 B. Nuthakki, T. L. Greaves, I. Krodziewska, A. Weerawardena, M. Burgar, R. J. Mulder and C. J. Drummond, *Aust. J. Chem.*, 2007, **60**, 21–28.
850
851
- 852 29 K. Richter, T. Bäcker and A.-V. Mudring, *Chem. Commun. (Camb.)*, 2009, 301–303.
853
- 854 30 H. Beyer and W. Walter, *Lehrbuch der Organischen Chemie*, 1988, S. Herzel Verlag, Stuttgart, p. 56.
855
- 856 31 A. Zicmanis, S. Pavlovica, E. Gzibovska, P. Mekss, and M. Klavins, *Latvian J. Chem*, 2010, **49**, 269–277.
857
- 858 32 P. Bharmoria, T. J. Trivedi, A. Pabbathi, A. Samantac and A. Kumar, *Phys. Chem. Chem. Phys.*, 2015, **17**, 10189–10199.
859
860
- 861 33 K. Shimojo, N. Kamiya, F. Tani, H. Naganawa, Y. Naruta and M. Goto, *Anal. Chem*, 2006, **78**, 7735–7742.
862
863
- 864 34 G. S. Zakharova, I. V. Uporov and V. I. Tishkov, *Biochem. Biokhimiia*, 2011, **76**, 1391–401.
865
- 866 35 E. H. Yu and K. Scott, *Energies*, 2010, **3**, 23–42.
- 867 36 R. Vazquez-Duhalt, *J. Mol. Catal. B: Enzym.*, 1999, **7**, 241–249.
868
- 869 37 R. W. Noble and Q. H. Gibson, *J. Biol. Chem.*, 1970, **245**, 2409–2413.
870
- 871 38 M. Patila, I. V. Pavlidis, E. K. Diamanti, P. Katapodis, D. Gournis and H. Stamatis, *Process Biochem.*, 2013, **48**, 1010–1017.
872
873
- 874 39 Y.M. Lee, O.Y Kwon, I.K. Yoo and K.G. Ryu, *J. Microbiol. Biotechnol.*, 2007, **17**, 600–603.
875
- 876 40 S. M. Sunil, P .S. Renuka, K. Pruthvi, M. Swetha, S. Malini, and S. M. Veena, *Enzyme Research*, 2011, **2011**, 7 pages.
877
878
- 879 41 J. R. L. Walker, *Biochem. Education*, 1992, **20**, 42–43.
880
- 881 42 J. A. Laszlo and D. L. Compton, *J. Mol. Catal. B Enzym.*, 2002, **18**, 109–120.
882
- 883 43 J. A. Villegas, A. G. Mauk and R. Vazquez-Duhalt, *Chem. Biol.*, 2000, **7**, 237–244.
884

- 885 44 R. Vazquez-Duhalt, K. M. Semple, D. W. S. Westlake and P. M. Fedorak, *Enzyme Microb. Technol.*, 1993, **15**, 936-943.
- 886
887
- 888 45 I. V. Pavlidis, D. Gournis, G. K. Papadopoulos and H. Stamatis, *J. Mol. Catal. B Enzym.*, 2009, **60**, 50-56.
- 889
890
- 891 46 R. Vazquez-Duhalt, D.W.S Westlake and P.M Fedorak, *Appl. Microbiol. Bioetchnol.*, 1995, **42**, 675-681.
- 892
893
- 894 47 S. K. Khare and M. Nakajima, *Food Chem.*, 2000, **68**, 153-157.
- 895
- 896 48 A. Romero, A. Santos, J. Tojo, A. Rodríguez, *J. Hazard. Mater.*, 2008, **151**, 268-273.
- 897
- 898 49 L. Rehmann, E. Ivanova, J. L. Ferguson, H. Q. N. Gunaratne, K. R. Seddon and G. M. Stephens, *Green Chem.*, 2012, **14**, 725.
- 899
900
- 901 50 K. Fujita, D. R. MacFarlane, M. Forsyth, M. Yoshizawa-Fujita, K. Murata, N. Nakamura and H. Ohno, *Biomacromolecules*, 2007, **8**, 2080-2086.
- 902
903
- 904 51 M. Bihari, T. P. Russell and D. a Hoagland, *Biomacromolecules*, 2010, **11**, 2944-2948.
- 905
- 906 52 W. Wei and N. D. Danielson, *Biomacromolecules*, 2011, **12**, 290-297.
- 907
- 908 53 A. P. M. Tavares, O. Rodriguez and E. Macedo, *Biotechnol. Bioeng.*, 2008, **101**, 201-207.
- 909
- 910 54 G. Hinckley, V.V. Mozhaev, C. Budde and Y.L. Khmel'nitsky, *Biotechnol. Lett.*, 2002, **24**, 2083-2087.
- 911
912
- 913 55 M. López-Pastor, A. Domínguez-Vidal, M. J. Ayora-Cañada, B. Lendl and M. Valcárcel, *Microchem. J.*, 2007, **87**, 93-98.
- 914
915
- 916 56 W.-Y. Lou, M.-H. Zong, Y.-Y. Liu and J.-F. Wang, *J. Biotechnol.*, 2006, **125**, 64-74.
- 917
- 918 57 H. Zhao, S. Campbell, J. Solomon, Z. Song, and O. Olubajo, *Chin. J. Chem.* 2006, **24**, 580-584.
- 919
- 920 58 Z. Yang, *J. Biotechnol.*, 2009, **144**, 12-22.
- 921
- 922 59 J.-Q. Lai, Z. Li, Y.-H. Lü and Z. Yang, *Green Chem.*, 2011, **13**, 1860.
- 923
924
- 925 61 K. D. Collins, *Methods*, 2004, **34**, 300-311.
- 926 62 K. Hernandez, A. Berenguer-Murcia, R.C. Rodrigues and R. Fernandez-Lafuente, *Curr. Org. Chem.*, 2012, **16**, 2652-2672.
- 927
928
- 929 63 L. Mao, S. Luo, Q. Huang and J. Lu, *Scientific Reports*, 2013, **3**:3126 7 pages.
- 930
- 931 64 R. Nakajima and I. Yamazaki, *J. Biol. Chem.*, 1980, **255**, 2067-2071.
- 932
- 933 65 J. N. Rodríguez-López, J. Hernández-Ruiz, F. García-Cánovas, R. N. F. Thorneley, M. Acosta, and M. B. Arnao, *J. Biol. Chem.*, 1997, **272**, 5469-5476.
- 934
935
- 936 66 R. M. Lau, M. J. Sorgedraeger, G. Carrea, F. Van Rantwijk, F. Secundo, R. A. Sheldon, B. L. Delft, V. M. Bianco and R. Sheldon, *Green Chem.*, 2004, **6**, 483-487.
- 937
938
939
- 940 67 J. Mc Murry, in *Organic Chemistry*, 7th Edn, 2008, ch 24, pp. 921-924.
- 941
- 942 68 J. O. Speare and T. S. Rush, *Biopolymers*, 2003, **72**, 193-204.
- 943
- 944 69 S. J. Prestrelski, N. Tedeschi, T. Arakawa, and J. F. Carpenter, *Biophys. J.*, 1993, **65**, 661-671.
- 945
- 946 70 F. Secundo, G. L. Barletta, E. Dumitriu, and G. Carrea, *Biotechnol. Bioeng.*, 2007, **97**, 12-18.
- 947
- 948 71 A. A. Tziaila, I. V Pavlidis, M. P. Felicissimo, P. Rudolf, D. Gournis and H. Stamatis, *Bioresour. Technol.*, 2010, **101**, 1587-1594.
- 949
950
- 951 72 G. W. Bushnell, G. V. Louie and G. D. Brayer, *J. Mol. Biol.*, 1990, **214**, 585.
- 952
- 953 73 A. Natalello, D. Ami, S. Brocca, M. Lotti and S. M. Doglia, *Biochem. J.* 2005, **385**, 511-517.
- 954
- 955 74 B. Mena, M. Herrero, V. Rives, M. Lavrenko, D. K. Eggers, *Biomaterials*, 2008, **29**, 2710-2718.
- 956
- 957 75 I. V. Pavlidis, T. Vorhaben, D. Gournis, G. K. Papadopoulos, U. T. Bornscheuer and H. Stamatis, *J. Nanopart. Res.*, 2012, **14**, 842.
- 958
959
- 960 76 S. Oellerich, H. Wackerbarth and P. Hildebrandt, *Eur. Biophys. J.*, 2003, **32**, 599-613.
- 961
- 962 77 Y. Kohno, N. Nakamura and H. Ohno, *Aust. J. Chem.*, 2012, **65**, 1548.
- 963
- 964 78 K. Fujita, M. Forsyth, D. R. MacFarlane, R. W. Reid and G. D. Elliott, *Biotechnol. Bioeng.*, 2006, **94**, 1209-13.
- 965
966

Journal Name					
967	79	M. Hulko, I. Hospach, N. Krasteva and G. Nelles, <i>Sensors</i> 2011, 11 , 5968-5980.	1006	96	G. Quijano, A. Couvert, A. Amrane, G. Darracq, C. Couriol, P. Le Cloirec, L. Paquin and D. Carrie, <i>Chem. Eng. J.</i> 2011, 174 , 27-32.
968			1007		
			1008		
969	80	F. Sinibaldi, B. D. Howes, G. Smulevich, C. Ciaccio, M. Coletta, and R. Santucci. <i>J. Biol. Inorg. Chem.</i> , 2003, 8 , 663–670	1009	97	O. Barbosa, R. Torres, C. Ortiz, A. Berenguer-Murcia, R.C. Rodrigues and R. Fernandez-Lafuente, <i>Biomacromol.</i> , 2013, 14 , 2433-2462.
970			1010		
971			1011		
972	81	R. A. Scott and A. G. Mauk, in <i>Cytochrome C. A multidisciplinary approach</i> . Sausalito, 1996, CA: University Science Books.	1012	98	R.C. Rodrigues, C. Ortiz, A. Berenguer-Murcia, R. Torres, and R. Fernández-Lafuente, <i>Chem. Soc. Rev.</i> , 2013, 42 , 6290-6307.
973			1013		
974			1014		
975	82	Y. P. Myer, <i>Biochemistry</i> , 1968, 7 , 765–776.	1015	99	P. Lozano, J.M. Bernal and A. Navarro, <i>A. Green Chem.</i> , 2012, 14 , 3026-3033.
976	83	R. W. Woody and M. C. Hsu, <i>J. Am. Chem. Soc.</i> , 1971, 93 , 3515–25.	1016		
977					
978	84	G. A. Baker and W. T. Heller, <i>Chem. Eng. J.</i> , 2009, 147 , 6–12.	1017	100	D.F. Izquierdo, M. Yates, P. Lozano, M.I. Burguete, E. Garcia-Verdugo and S.V Luis, <i>React. Funct. Polym.</i> , 2014, 85 , 20-27.
979			1018		
			1019		
980	85	K. Fujita and H. Ohno, <i>Biopolymers</i> , 2010, 93 , 1093-1099.	1020		
981					
			1021		
982	86	J. Gong, P. Yao, H. W. Duan, M. Jiang, S. H. Gu and L. Chunyu, <i>Biomacromolecules</i> , 2003, 4 , 1293–1300.	1022		
983					
984	87	Y. G Thomas, R. A. Goldbeck and D. S. Kliger, <i>Biopolymers</i> , 2000, 57 , 29–36.	1023		
985					
			1024		
986	88	N. Chahbane, D. Lenoir, S. Souabi, T. J. Collins and K.-W. Schramm, <i>CLEAN – Soil, Air, Water</i> , 2007, 35 , 459–464.	1025		
987					
988					
			1026		
989	89	E. Abadulla, T. Tzanov, S. Costa, K. H. Robra, A. Cavaco-Paulo and G. M. Gubitz, <i>Appl. Environ. Microb.</i> , 2000, 66 , 3357–3362.	1027		
990					
991					
			1028		
992	90	A. Zille, T. Tzanov, G. M. Gubitz, and M. Cavaco-Paulo, <i>Biotechnol. Lett.</i> , 2003, 25 , 1473–1477.	1029		
993					
			1030		
994	91	C. Viral, S. Rohit, S. Dharmendra, M. Hasmukh and R. M. V. Bharatkumar, <i>Enzyme Microb. Tech. J.</i> , 2005, 36 , 327-332.	1031		
995					
996					
997	92	D. Salvachúa, A. Prieto, Á. T. Martínez and M. J. Martínez. <i>Appl. Environ. Microbiol.</i> , 2013, 79 , 4316–4324.			
998					
999					
1000	93	J. M. Lanzafame, A. A. Muentner and D. V. Brumbaugh, <i>Chem. Phys.</i> , 1996, 210 , 79.			
1001					
1002	94	M. T. Garcia, N. Gathergood and P. J. Scammells, <i>Green Chem.</i> , 2005, 7 , 9-14.			
1003					
1004	95	A. S. Wells and V. T. Coombe, <i>Org. Process Res. Dev.</i> 2006, 10 , 794-798.			
1005					

Figure Captions

Fig. 1. Structure of ILs used in the present study

Fig. 2. Relative peroxidase activity of cyt c for the oxidation of guaiacol in the presence of various amounts of hydroxyl ammonium-based ILs. As 1.0 is indicated the peroxidase activity of cyt c in 50 mM phosphate buffer pH 7.0. Initial reaction rate of the activity of cyt c in buffer is 10 $\mu\text{M}/\text{min}$.

Fig. 3. Effect of the concentrations of hydroxyl ammonium-based ILs on the catalytic efficiency of cytochrome c for the oxidation of guaiacol with H_2O_2 . The black line represents the ratio of $V_{\text{max}}^{\text{app}}/K_m^{\text{app}}$ of cyt c in buffer aqueous solution.

Fig. 4. Stability of cyt c in buffer and 30, 45 and 60 % v/v aqueous solutions of hydroxyl ammonium-based ILs, after incubation for 15 min with 1 mM H_2O_2 at 30 $^\circ\text{C}$. As 100% is indicated the activity at $t = 0$ min.

Fig. 5. UV-visible spectra (300-600 nm) of cyt c in 50 mM phosphate buffer, pH 7.0 and in the presence of 60% (v/v) ILs. The insets show the absorption spectra of the media (60% v/v ILs).

Fig. 6. Absorption spectra of cyt c at the charge transfer band (695 nm) in phosphate buffer 50 mM, pH 7.0 and in the presence of 60% (v/v) ILs.

Fig. 7. Soret region CD spectrum of cyt c in 50 mM phosphate buffer, pH 7.0 and in the presence of 60% (v/v) aqueous solution of HMEAF.

Fig. 8. Cyt c-catalyzed decolorization of pinacyanol chloride with H_2O_2 in phosphate buffer 50 mM, pH 7.0 and in the presence of various amounts (15-75 % v/v) of ILs a) HMEAF, b) HDMEAF, c) BHEAF and d) HEAF.

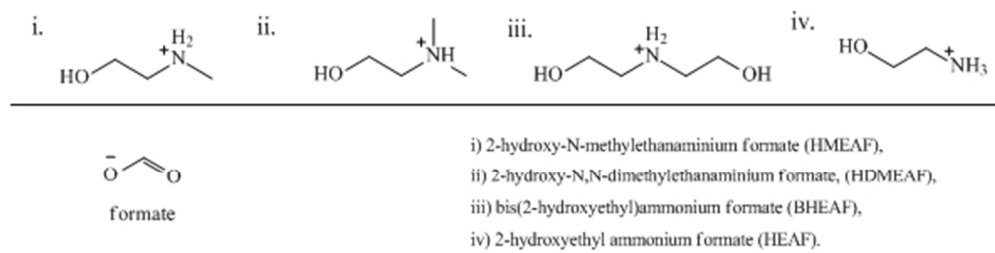


Fig. 1. Structure of ILs used in the present study

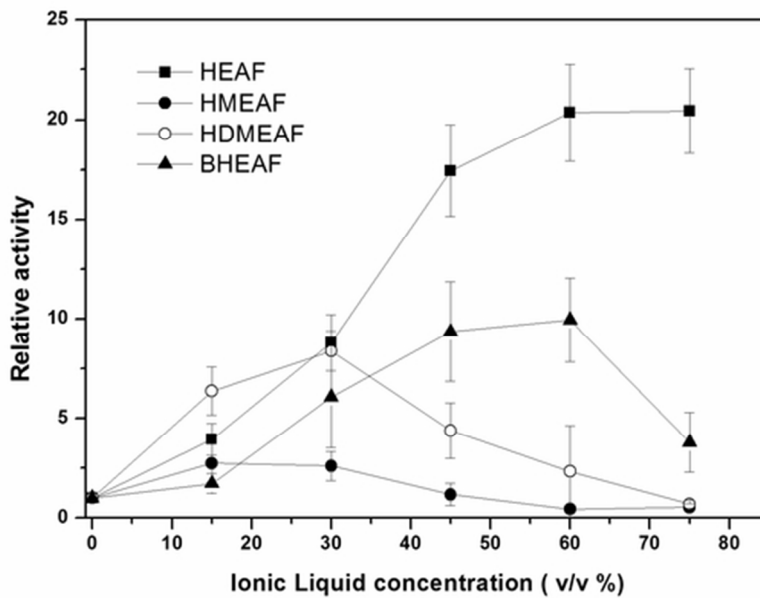
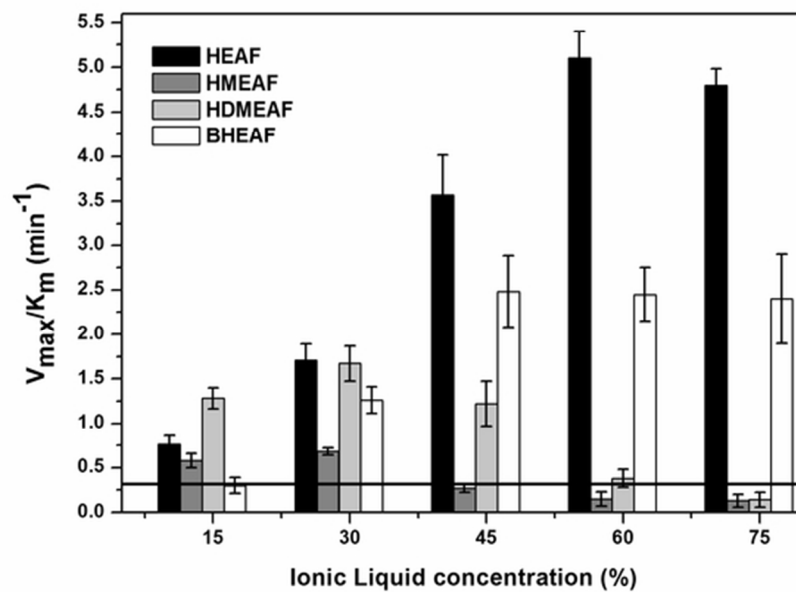
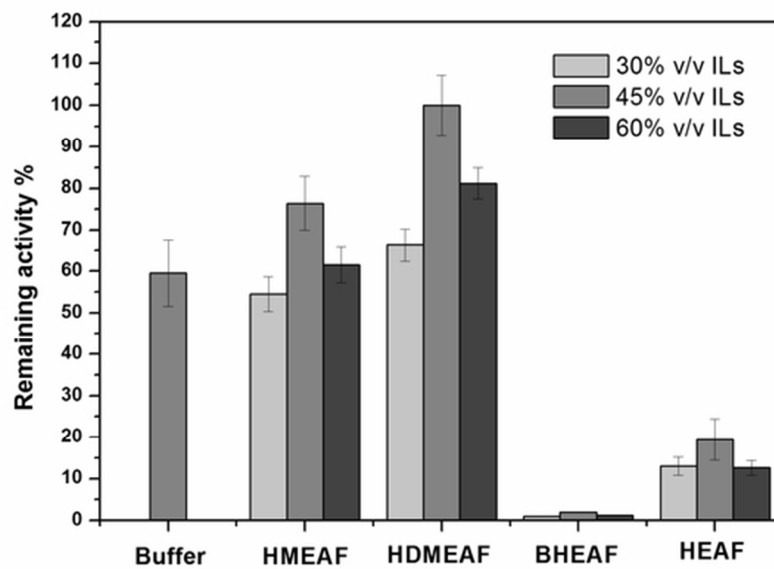


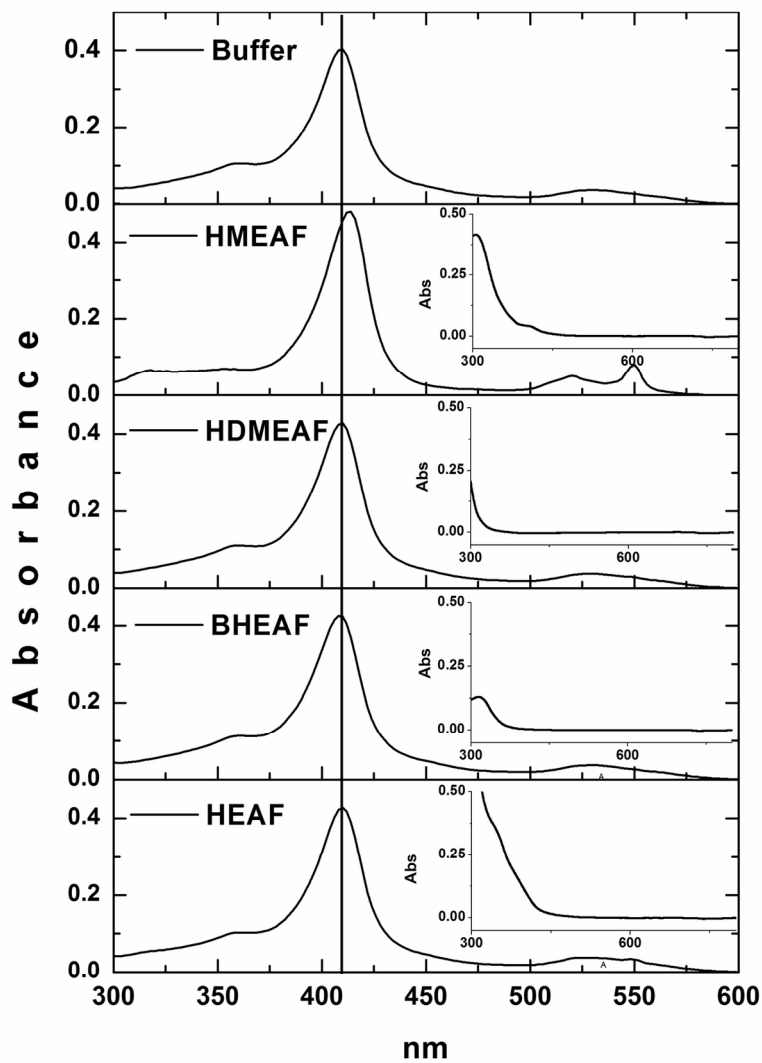
Fig. 2. Relative peroxidase activity of cyt c for the oxidation of guaiacol in the presence of various amounts of hydroxyl ammonium-based ILs. As 1.0 is indicated the peroxidase activity of cyt c in 50 mM phosphate buffer pH 7.0. Initial reaction rate of the activity of cyt c in buffer is 10 $\mu\text{M}/\text{min}$
55x38mm (300 x 300 DPI)



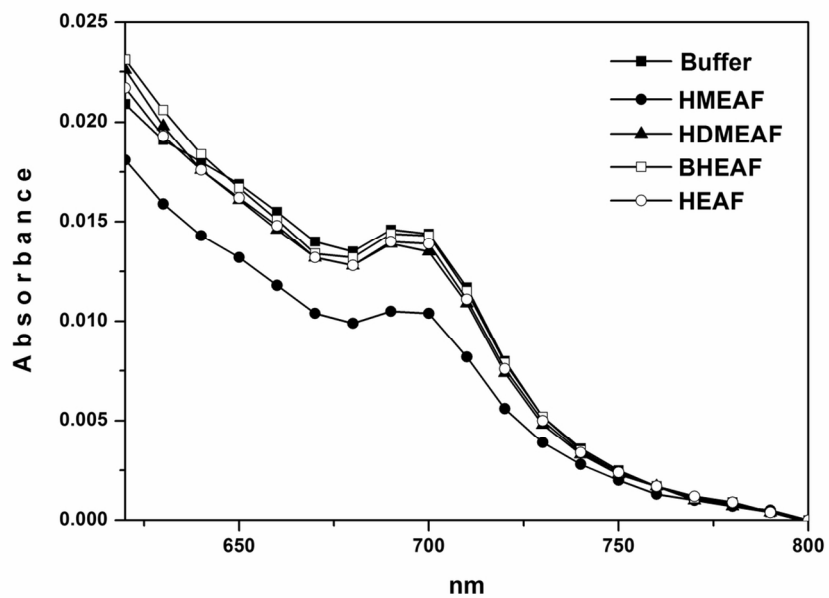
Effect of the concentrations of hydroxyl ammonium-based ILs on the catalytic efficiency of cytochrome c for the oxidation of guaiacol with H_2O_2 . The black line represents the ratio of V_{max}^{app}/K_m^{app} of cyt c in buffer aqueous solution
57x39mm (300 x 300 DPI)



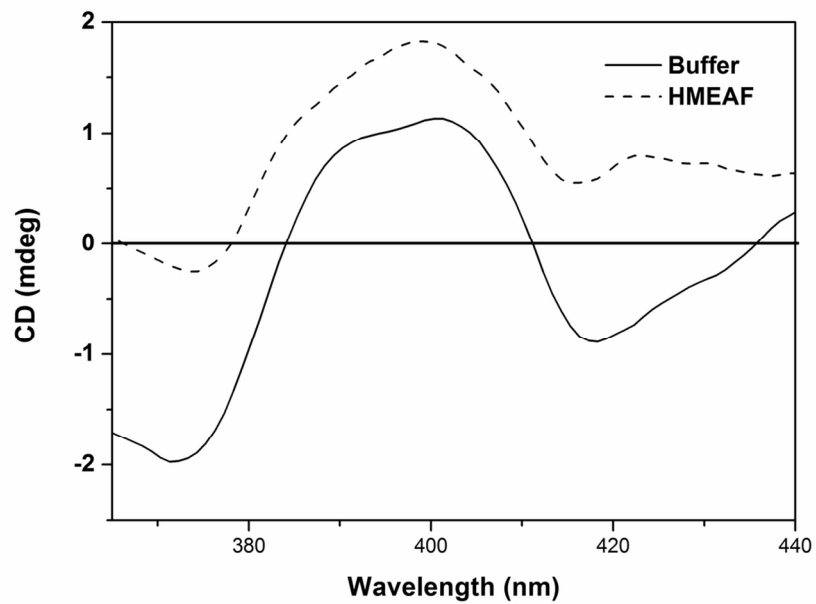
Stability of cyt c in buffer and 30, 45 and 60 % v/v aqueous solutions of hydroxyl ammonium-based ILs, after incubation for 15 min with 1 mM H₂O₂ at 30 °C. As 100% is indicated the activity at t = 0 min.
57x39mm (300 x 300 DPI)



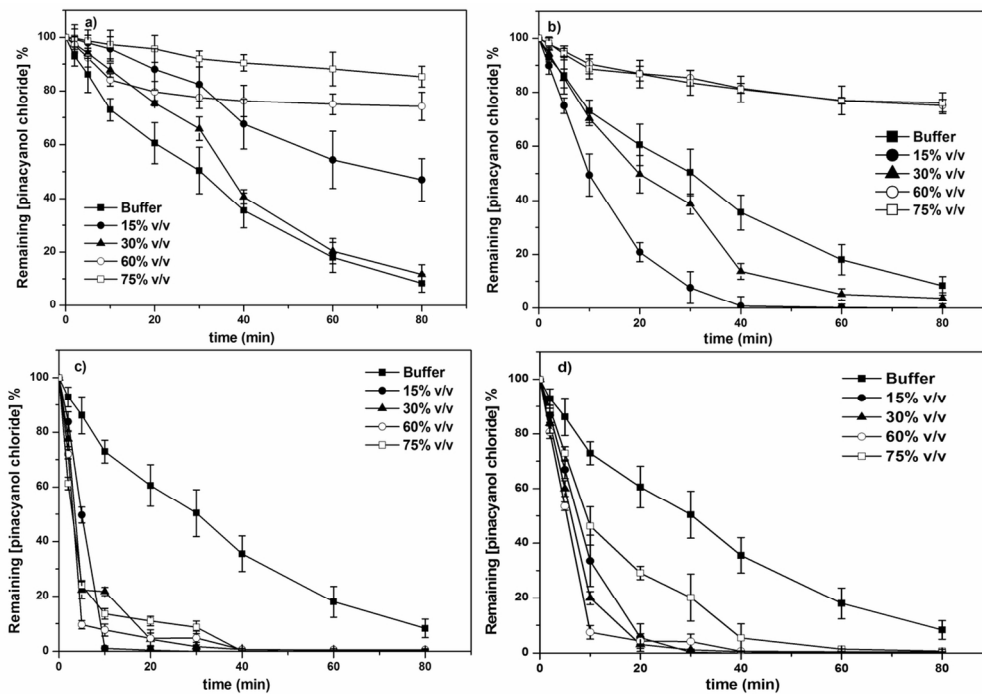
UV-visible spectra (300-600 nm) of cyt c in 50 mM phosphate buffer, pH 7.0 and in the presence of 60% (v/v) ILs. The insets show the absorption spectra of the media (60% v/v ILs).
119x172mm (300 x 300 DPI)



Absorption spectra of cyt c at the charge transfer band (695 nm) in phosphate buffer 50 mM, pH 7.0 and in the presence of 60% (v/v) ILs.
57x39mm (600 x 600 DPI)



Soret region CD spectrum of cyt c in 50 mM phosphate buffer, pH 7.0 and in the presence of 60% (v/v) aqueous solution of HMEAF
57x39mm (600 x 600 DPI)



Cyt c-catalyzed decolorization of pinacyanol chloride with H_2O_2 in phosphate buffer 50 mM, pH 7.0 and in the presence of various amounts (15-75 % v/v) of ILs a) HMEAF, b) HDMEAF, c) BHEAF and d) HEAF
118x82mm (300 x 300 DPI)

Table 2. Activation energy E_a for the oxidation of guaiacol catalyzed by cyt c in various ILs (30% v/v).

<i>Activation Energy E_a (kcal/mol)</i>				
<i>Buffer</i>	BHEAF	HDMEAF	HMEAF	HEAF
1.28	1.17	1.19	0.67	0.58

Table 3. Correlation coefficient (r) between the ATR-FTIR spectra of cyt c dissolved in 50 mM sodium phosphate buffer, pH 7.0 and in 30% (v/v) aqueous solutions of ILs. $\Delta\alpha$ -helix estimation (%) is the difference between the percentages of α -helix content of cyt c in 30% (v/v) ILs compared to that in buffer calculated by ATR-FTIR analysis in Amide I region.

Ionic Liquid	r	$\Delta\alpha$-helix (%)
HMEAF	0.97	+0.80
HDMEAF	0.93	+2.50
BHEAF	0.98	-0.68
HEAF	0.94	+1.72

Table 4. Reaction rates of the cyt c-catalyzed decolorization of pinacyanol chloride with H₂O₂ in phosphate buffer 50 mM, pH 7.0 and in the presence of various amounts of hydroxyl-ammonium ILs.

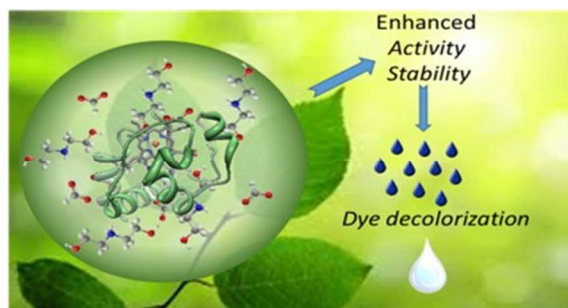
% v/v ILs	Decolorization rate ($\mu\text{M min}^{-1}$)			
	HMEAF	HDMEAF	BHEAF	HEAF
0	3.9	3.9	3.9	3.9
15	0.9	7.8	11.3	9.9
30	1.8	4.0	14.0	12.5
60	2.5	1.5	17.4	14.5
75	0.4	1.3	18.6	8.0

Table 5. (%) Biodegradability assessment of the hydroxyl ammonium ILs.

Ionic Liquid	(%) Biodegradation *
2-HEAF	58.9
HMEAF	55.0
HDMEAF	57.4
BHEAF	52.2

* The percentage biodegradation is calculated by dividing the specific carbonaceous BOD (CBOD) by the ultimate carbonaceous BOD (UCBOD). The **CBOD** value expresses the oxygen demand by microorganisms for degradation of the ILs within five days (only carbonaceous stage). CBOD is the BOD value (mg O₂/L) reading affected due to the drop of pressure in the water sample bottle, minus the BOD value reading affected due to the drop of pressure in the dilution water bottle (blank). The **UCBOD** value (mg O₂/L), expresses the oxygen demand by microorganisms for the ultimate degradation of the organic compound referring only to the conversion of organic carbon to carbon dioxide, water, and new microbial cellular constituents.

Hydroxyl ammonium ionic liquids are a biodegradable, non-toxic family of third generation ionic liquids with a beneficial effect on the catalytic efficiency of metalloproteins such as cytochrome c.



Electronic Supplementary Information

Hydroxyl ammonium ionic liquids as media for biocatalytic oxidations

Athena A. Papadopoulou,^α Andromachi Tzani,^β Dimitrios Alivertis,^α Maria H. Katsoura,^α Angeliki C. Polydera,^α Anastasia Detsi^β and Haralambos Stamatis^{α*}

^α *Department of Biological Applications and Technology, University of Ioannina, University Campus, 45110 Ioannina, Greece*

^β *Department of Chemical Sciences, Laboratory of Organic Chemistry, National Technical University of Athens, Heroon Polytechniou 9, Zografou Campus, 15780 Athens, Greece*

Corresponding Author: *E-mail: hstamati@cc.uoi.gr* (H. Stamatis)

URL: *<http://biotechlab.bat.uoi.gr/index.php/en/>*

Tel.: +30 26510 97116; fax: +30 26510 97343

Biodegradability test

Biodegradation is the natural process for the removal of organic substances from the environment. The determination of the biodegradability level of organic substances such as ILs is essential in order to estimate their environmental impact. Biodegradability assessment of ILs have been examined by measuring the Biochemical Oxygen Demand (BOD) [1],[2].

In this work, biodegradation tests were carried out according to a manometric method so as to determine the oxygen demand for the biochemical degradation of each organic substance after five days. VELP BOD manometric apparatus was used to measure the BOD of the IL inoculated samples. This method is based on the steady decrease of the pressure in a closed system as a result of oxygen consumption. The carbon dioxide which is produced is bounded by a strongly alkaline medium (KOH pellets above the solution) so as not to interfere with the final measurements. The nutrients prepared are:

- Ferric chloride hexahydrate: 0.25 g $\text{FeCl}_3 \cdot 6\text{H}_2\text{O}$ to a final volume of 1 L with distilled water.
- Calcium chloride anhydrous: 27.5 g CaCl_2 to a final volume of 1 L with distilled water.
- Magnesium sulfate heptahydrate: 22.5 g $\text{MgSO}_4 \cdot 7\text{H}_2\text{O}$ to a final volume of 1 L with distilled water.
- Phosphate salts solution (buffer): 8.5 g KH_2PO_4 , 21.7 g K_2HPO_4 , 33.4 g $\text{Na}_2\text{HPO}_4 \cdot 7\text{H}_2\text{O}$ and 1.7 g NH_4Cl to a final volume of 1 L with distilled water.

This method consists of filling each BOD flask with specific amount of IL, 135 mL aqueous solution of nutrients and 15 mL microorganisms. The seed source of microorganisms was mixed liquor which was taken from a secondary sedimentation tank of urban waste water of Psyttaleia sewage treatment plant in Greece. A blank solution was also prepared, containing only nutrients and mixed liquor.

In general, two stages of degradation take place during the BOD test, carbonaceous and nitrogenous but in this work only the carbonaceous demand taken into account and the BOD values will be reported as CBOD (degradation of the organic carbon). Inhibition of nitrogenous bacteria was achieved by a thiourea solution (2 g thiourea to a final volume of 1 L with distilled water) which was also added to BOD samples (0.5 mL of the solution in each flask). The samples were kept at $20 \pm 1^\circ\text{C}$ in darkness in tightly closed bottles for an incubation period of 5 days.

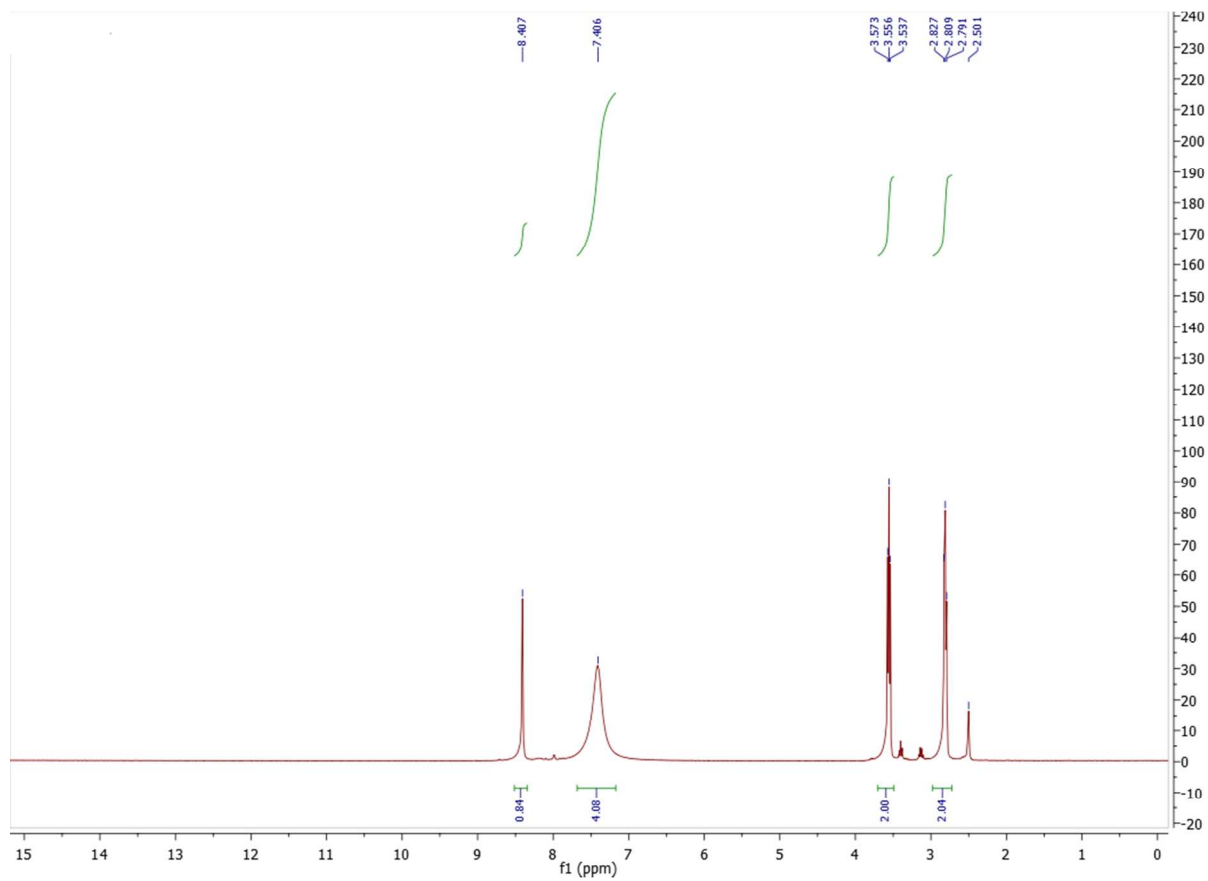


Fig. S1. ^1H NMR spectrum of 2-hydroxyethylammonium formate (HEAF).

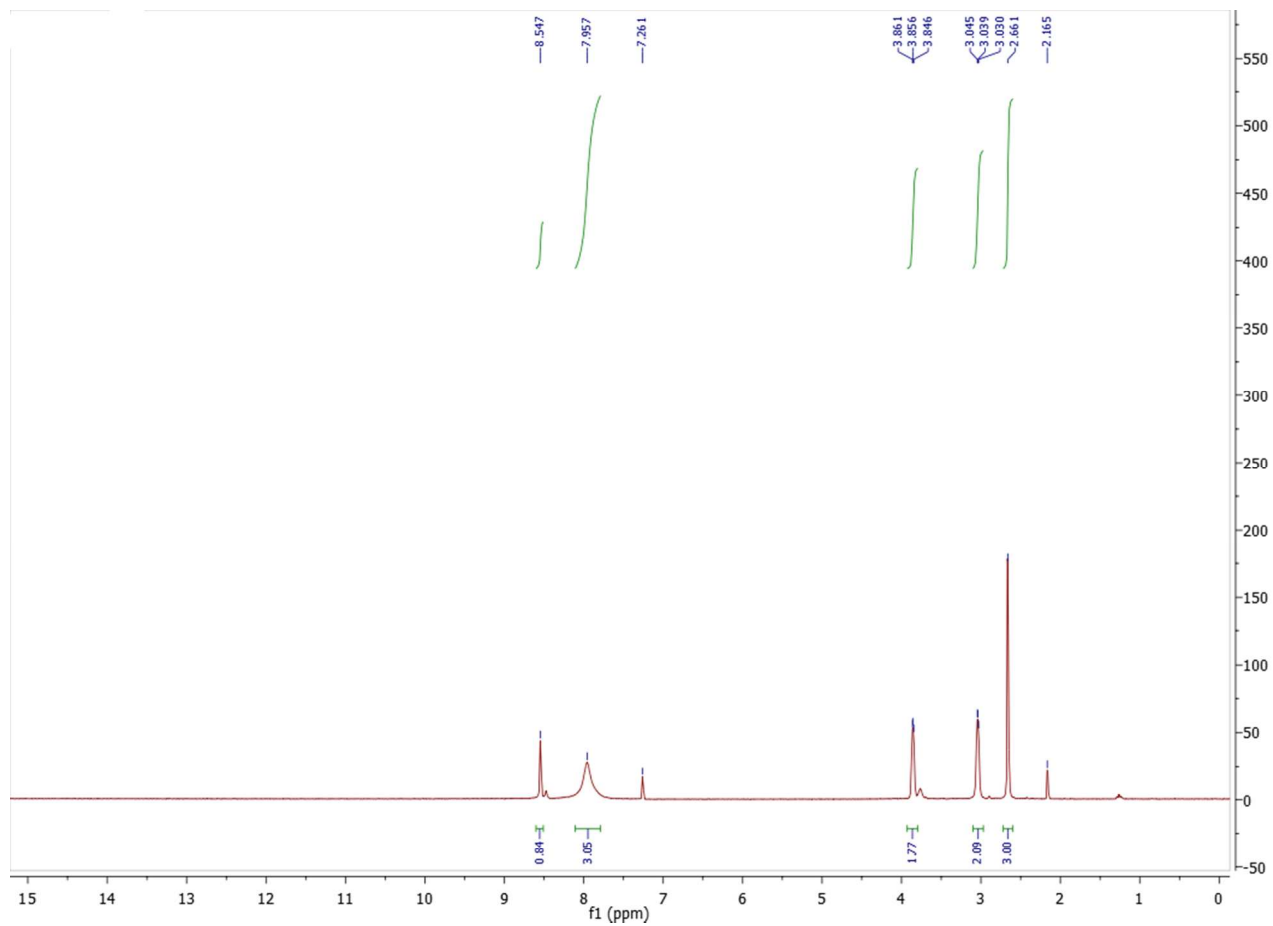


Fig. S2. ^1H NMR spectrum of 2-hydroxy-N-methylethanaminium formate (HMEAF).

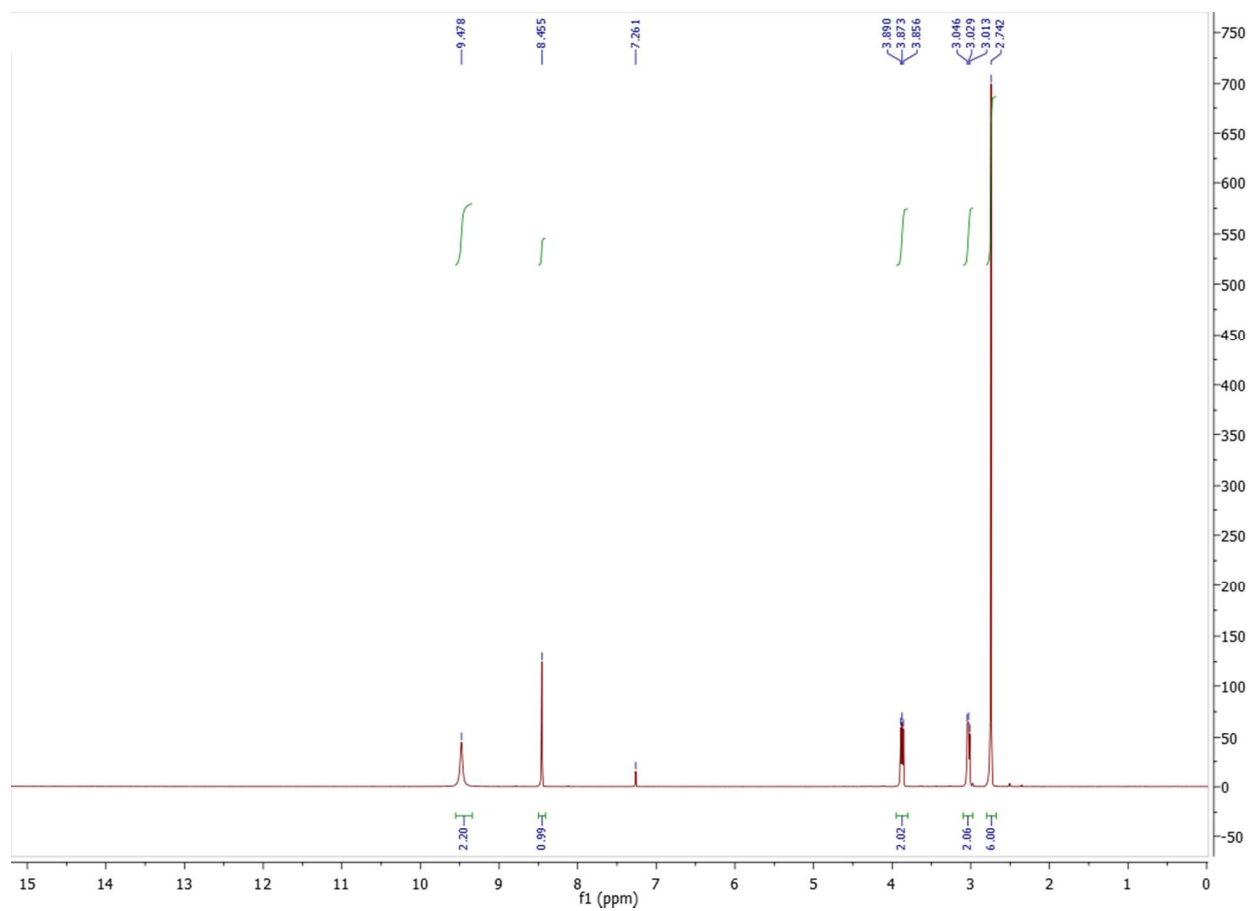


Fig. S3. ^1H NMR spectrum of 2-hydroxy-*N,N*-dimethylethanaminium formate (HDMEAF).

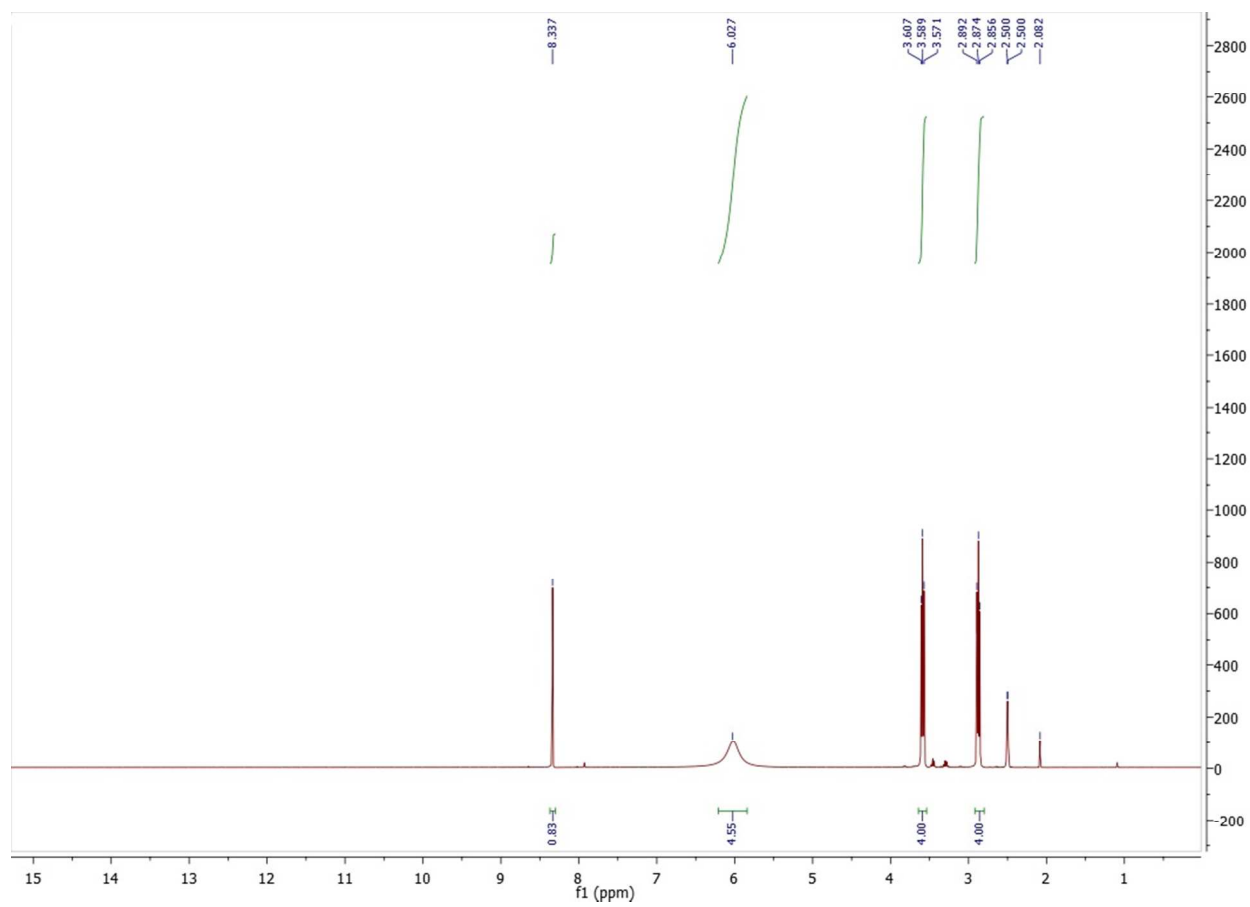


Fig. S4. ^1H NMR spectrum of *bis(2-hydroxyethyl)ammonium formate* (BHEAF).

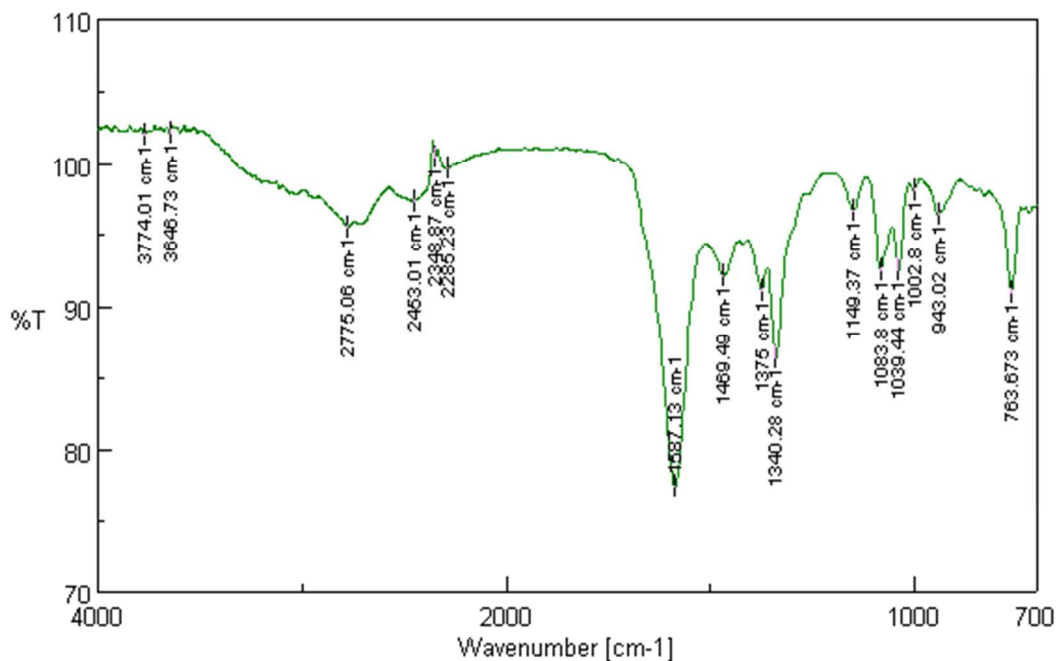


Fig. S5. ATR spectrum of 2-hydroxyethylammonium formate (HEAF).

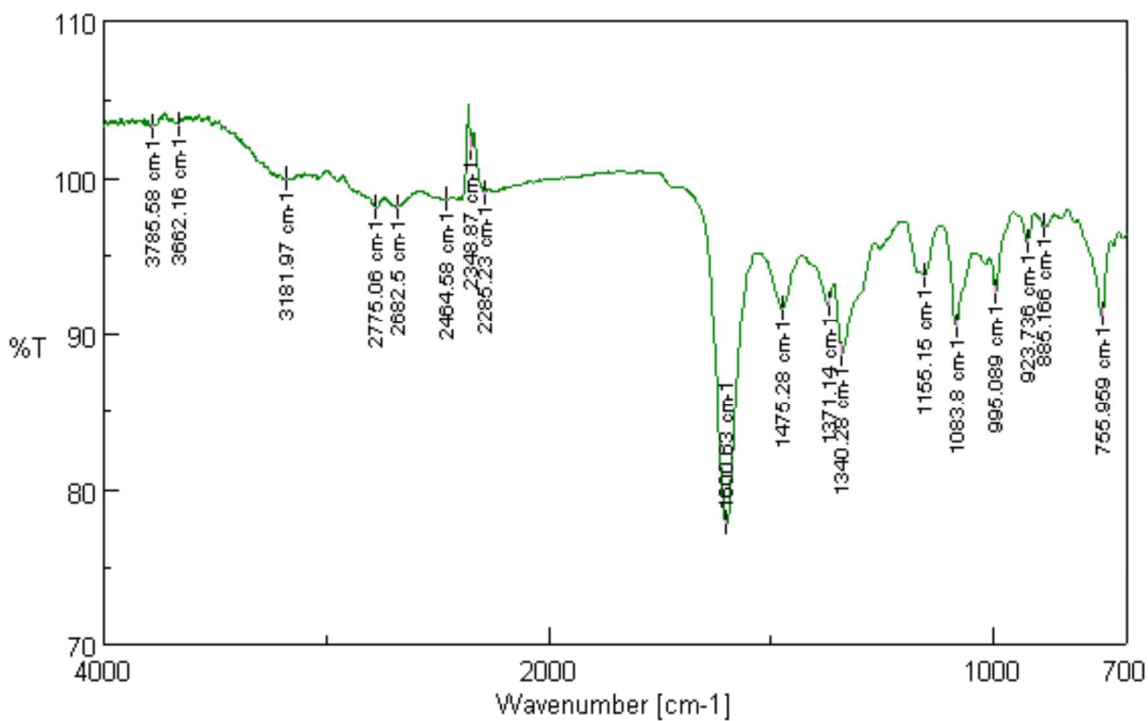


Fig. S6. ATR spectrum of 2-hydroxy-N,N-dimethylethanaminium formate (HDMEAF).

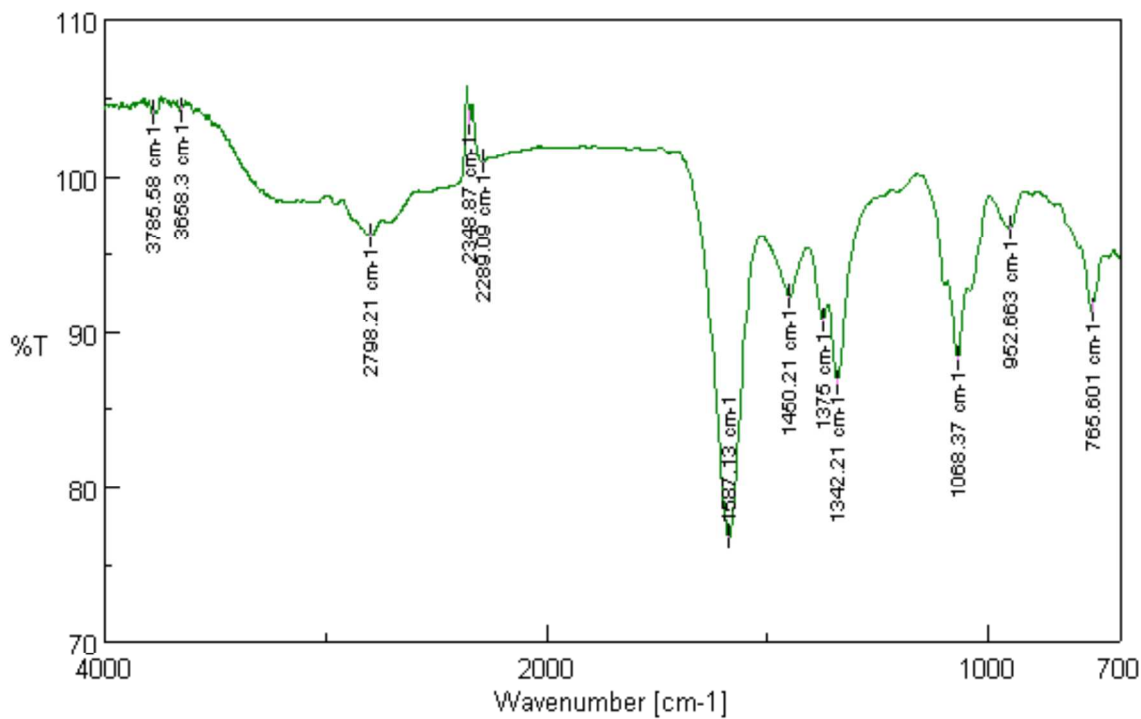


Fig. S7. ATR spectrum of bis(2-hydroxyethyl)ammonium formate (BHEAF)

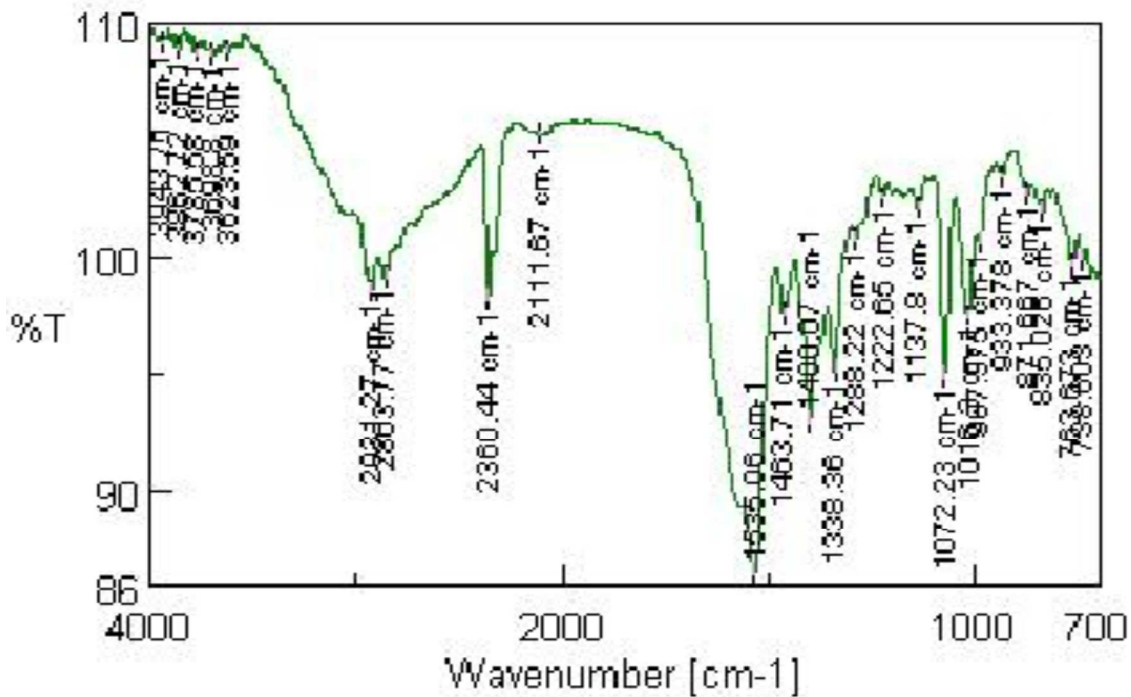


Fig. S8. ATR spectrum of 2-hydroxyethylammonium formate (HEAF):

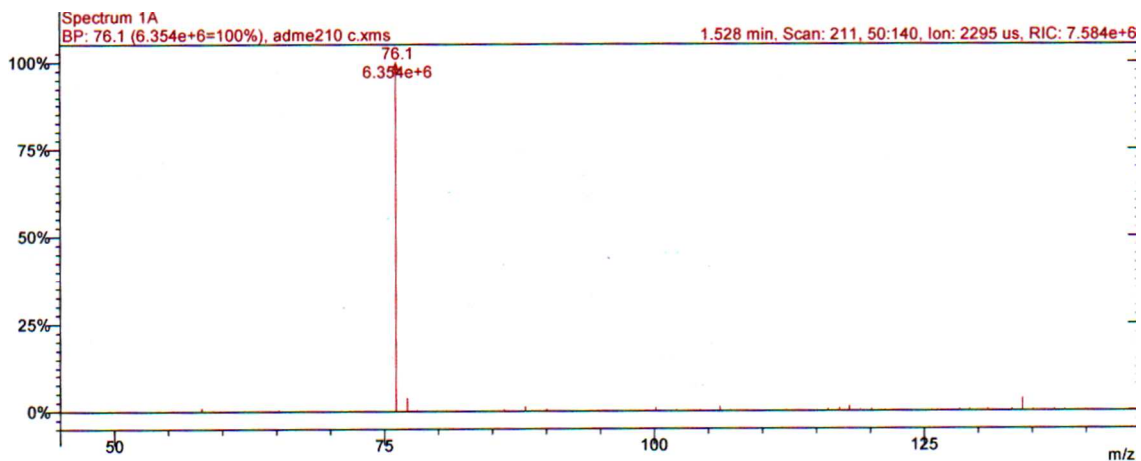


Fig. S9. MS spectrum of 2-hydroxy-N-methylethanaminium formate (HMEAF).

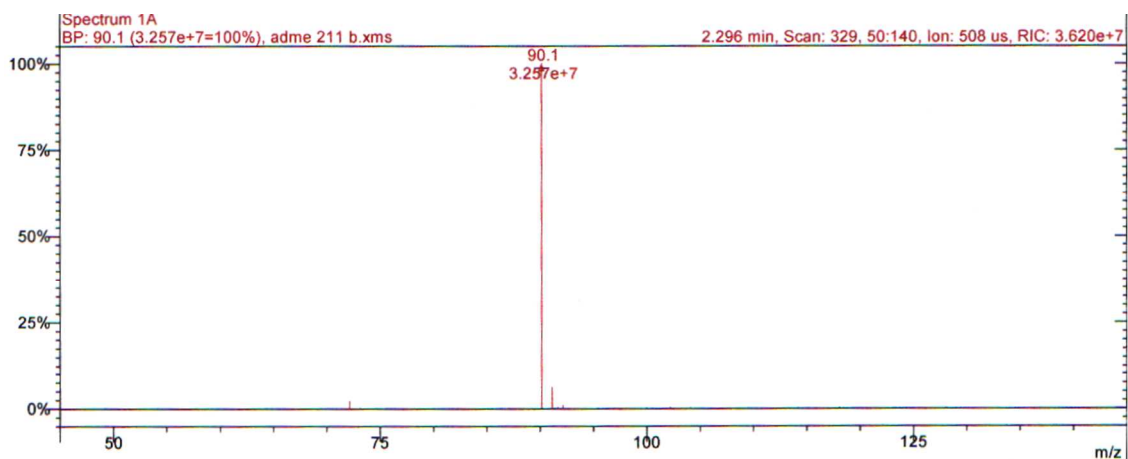


Fig. S10. MS spectrum of 2-hydroxy-N,N-dimethylethanaminium formate (HDMEAF).

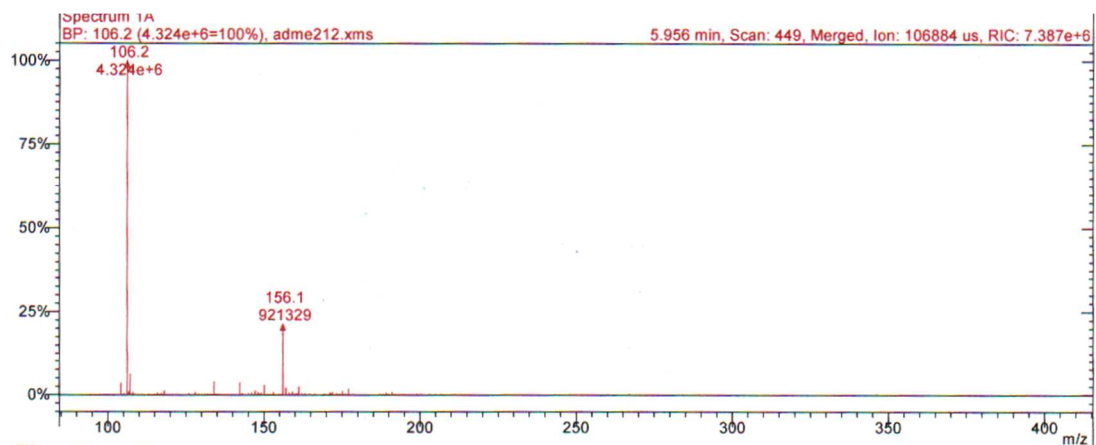


Fig. S11. MS spectrum of bis(2-hydroxyethyl)ammonium formate (BHEAF).

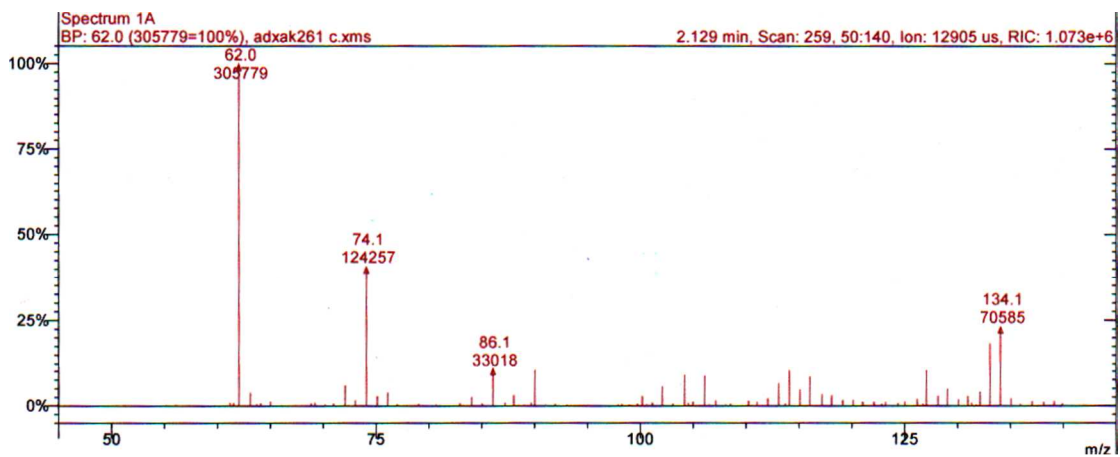


Fig. S12. MS spectrum of 2-hydroxyethylammonium formate (HEAF).

The UV–Vis spectroscopic measurements were performed on a double-beam UV-vis spectrophotometer (UV-1601 Shimadzu, Tokyo, Japan) in a standard 1 cm path length quartz cuvette.

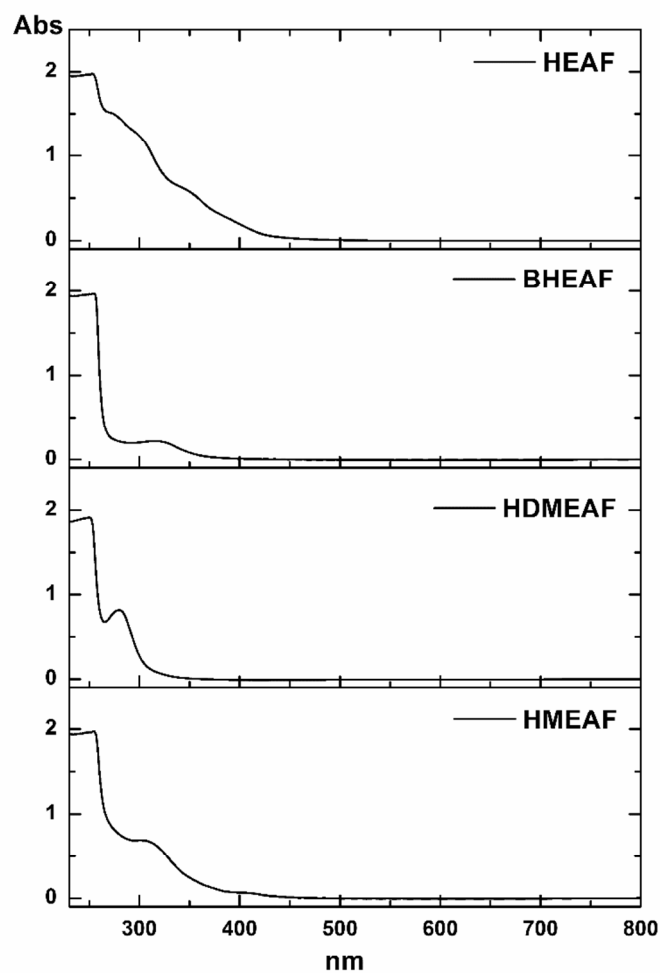


Fig. S13. UV-vis spectra (230-800 nm) of all ILs used in this study.

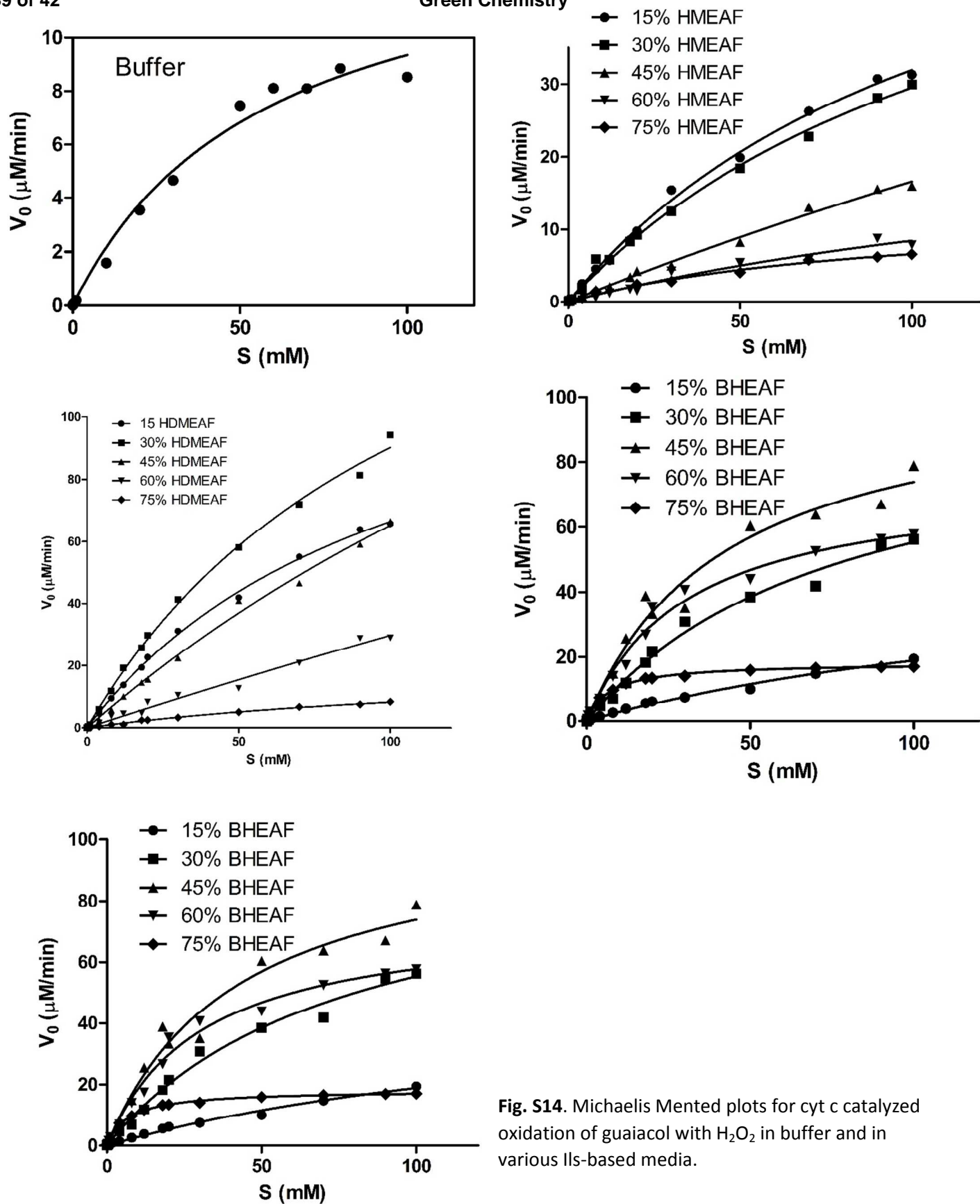


Fig. S14. Michaelis Mented plots for cyt *c* catalyzed oxidation of guaiacol with H_2O_2 in buffer and in various IIs-based media.

Table S1. Apparent kinetic parameters K_m^{app} (μM) and V_{max}^{app} ($\mu\text{M min}^{-1}$) of guaiacol oxidation with H_2O_2 by cyt c in the presence of various amounts of ILs (0-75% v/v).

% of IL in reaction medium (v/v)	HEAF		HMEAF		HDMEAF		BHEAF	
	K_m^{app}	V_{max}^{app}	K_m^{app}	V_{max}^{app}	K_m^{app}	V_{max}^{app}	K_m^{app}	V_{max}^{app}
0	58.6 ± 1.1	18.8 ± 2.5	58.6 ± 1.1	18.8 ± 2.5	58.6 ± 1.1	18.8 ± 2.5	58.6 ± 1.1	18.8 ± 2.5
15	93.3 ± 2.2	70.96 ± 2.9	120.3 ± 5.3	70.3 ± 4.2	107.2 ± 5.4	137.9 ± 5.9	173.2 ± 10.9	51.6 ± 3.5
30	110 ± 1.2	188.7 ± 8.5	63.3 ± 3.1	43.5 ± 3.6	117.2 ± 6.8	196.0 ± 9.8	77.5 ± 5.6	98.2 ± 6.8
45	111.1 ± 1.4	397.4 ± 10.8	118.2 ± 6.8	32.1 ± 3.9	88.7 ± 4.3	108.7 ± 7.3	42.2 ± 3.6	105.1 ± 12.1
60	45.2 ± 2.5	231.8 ± 12.8	113.5 ± 7.2	16.8 ± 2.8	281.2 ± 8.6	107.8 ± 6.4	30.8 ± 6.8	75.6 ± 9.8
75	34.3 ± 1.6	164.4 ± 19.3	99.3 ± 7.1	13.1 ± 1.2	143.2 ± 5.9	20.2 ± 3.6	7.6 ± 4.3	18.4 ± 2.3

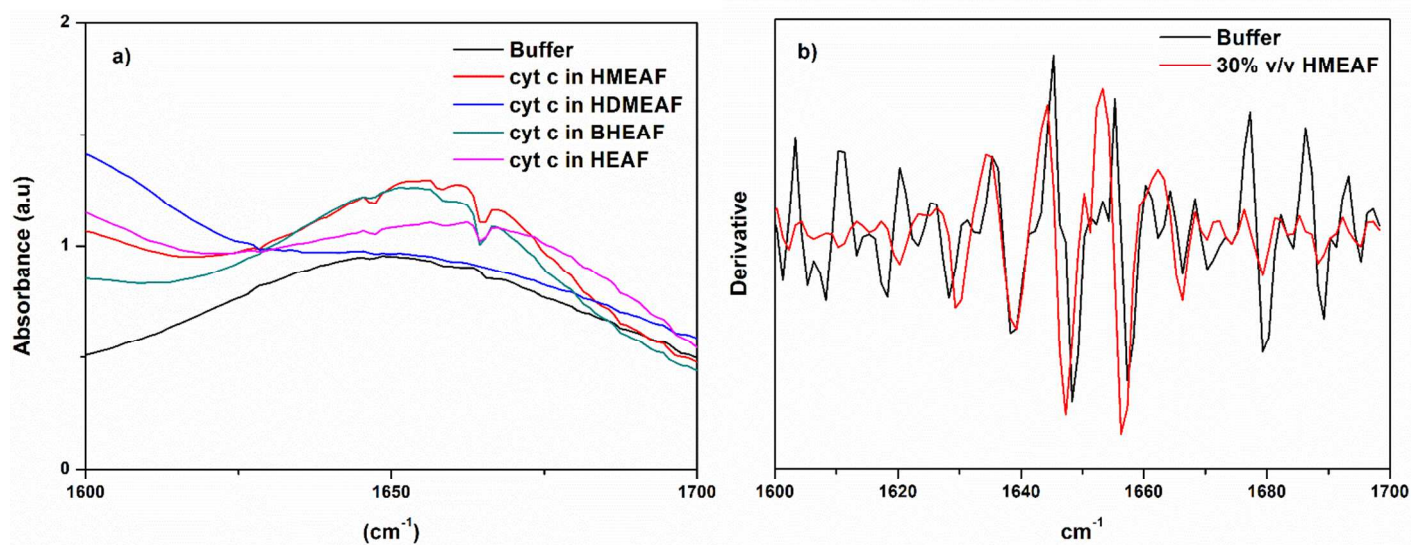


Fig. S15. a) Comparison of ATR spectra of the Amide I region of cyt c in 50 mM phosphate buffer pH 7.0 and 30% v/v of all ILs studied, b) Comparison of the second derivative spectra in the Amide I region of cyt c in 50mM phosphate buffer pH 7.0 and 30% v/v HMEAF.

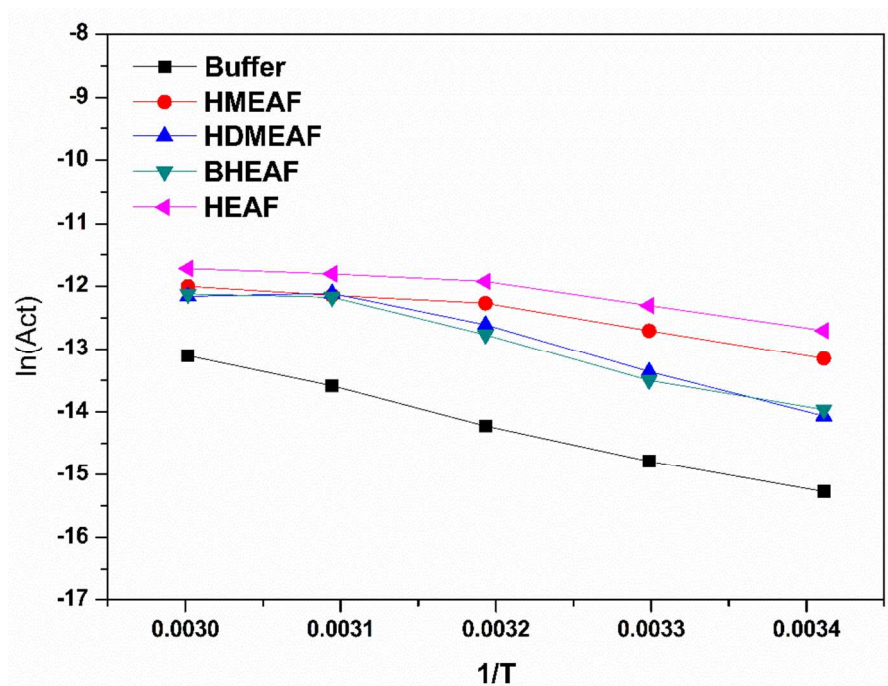


Fig. S16. Arrhenius plots of cyt c activity in buffer and all ILs studied.

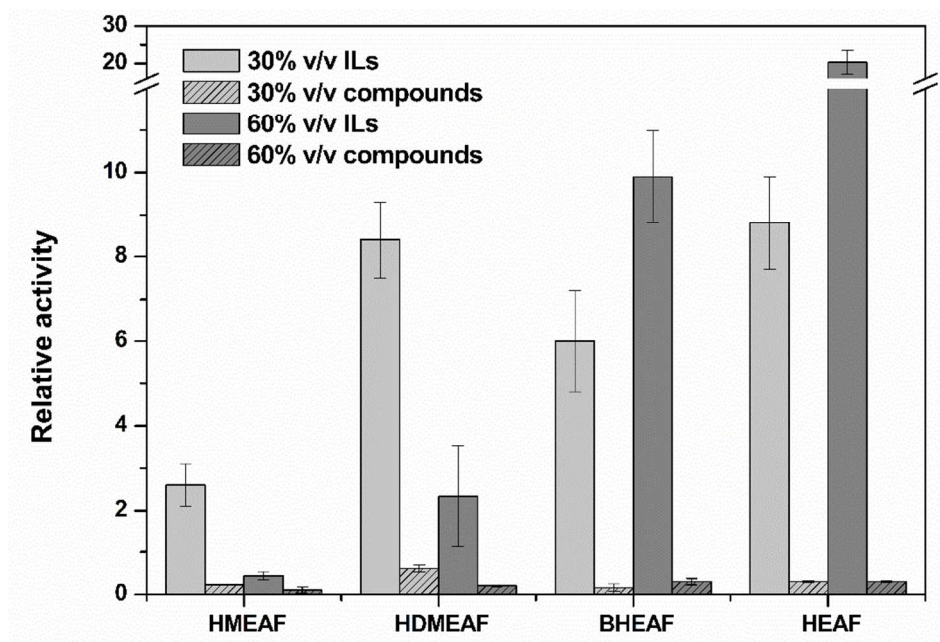


Fig. S17. Relative peroxidase activity of cyt c for the oxidation of guaiacol in the presence of various amounts of hydroxyl ammonium-based ILs and its equimolar amounts of individual components. As 1.0 is indicated the peroxidase activity of cyt c in 50 mM phosphate buffer pH 7.0. Initial reaction rate in buffer: 10 μ M/min.

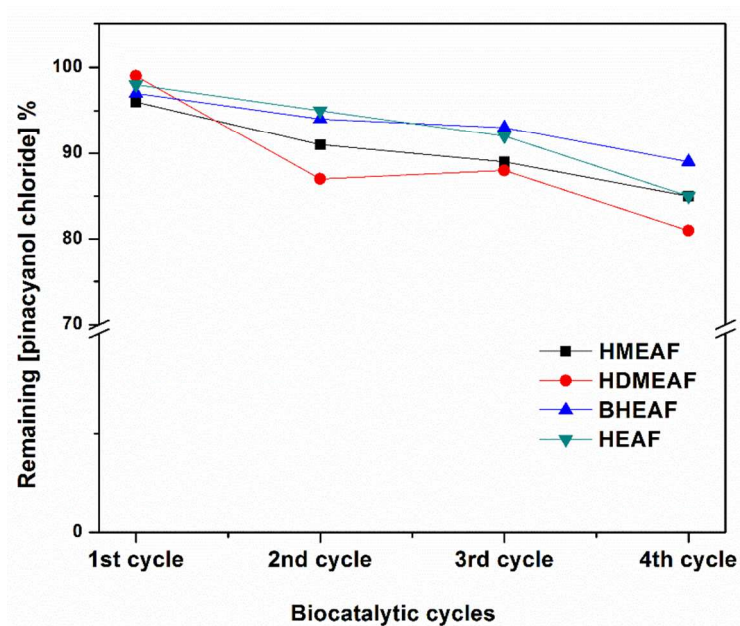


Figure S18. Recycle of ILs used as media in the decolorization of pinacyanol chloride catalyzed by immobilized cyt c.

References

- [1] A. Tzani, A. Douka, A. Papadopoulos, E.A. Pavlatou, E. Voutsas, A. Detsi, ACS Sustainable Chem. Eng. 1 (2013) 1180–1185.
- [2] A. Romero, A. Santos, J. Tojo, A. Rodríguez, J. Hazard. Mater. 151 (2008) 268–273.